

**THE ROLE OF CRUSTAL ANATEXIS AND MANTLE-DERIVED MAGMAS  
 IN THE GENESIS OF SYNOROGENIC HERCYNIAN GRANITES  
 OF THE LIVRADOIS AREA, FRENCH MASSIF CENTRAL**

FABIEN SOLGADI<sup>§</sup>

*Géologie et Gestion des Ressources Minérales et Energétiques, Université Henri Poincaré Nancy 1, BP 239, F-54506,  
 Vandoeuvre-lès-Nancy Cedex, France, and Sciences de la Terre, Département des Sciences Appliquées,  
 Université du Québec à Chicoutimi, Chicoutimi, Québec G7H 2B1, Canada*

JEAN-FRANÇOIS MOYEN

*Géologie et Gestion des Ressources Minérales et Energétiques, Université Henri Poincaré Nancy 1, BP 239, F-54506,  
 Vandoeuvre-lès-Nancy Cedex, France, and Department of Geology, Geography and Environmental Studies,  
 Stellenbosch University, Private Bag XI, Matieland, 7602, South Africa*

OLIVIER VANDERHAEGHE

*Géologie et Gestion des Ressources Minérales et Energétiques, Université Henri Poincaré Nancy 1, BP 239, F-54506,  
 Vandoeuvre-lès-Nancy Cedex, France*

EDWARD W. SAWYER

*Sciences de la Terre, Département des Sciences Appliquées, Université du Québec à Chicoutimi,  
 Chicoutimi, Québec G7H 2B1, Canada and Géologie et Gestion des Ressources Minérales et Energétiques,  
 Université Henri Poincaré Nancy 1, BP 239, F-54506, Vandoeuvre-lès-Nancy Cedex, France*

LAURIE REISBERG

*Laboratoire du C.R.P.G., 15, rue Notre Dame des Pauvres, BP20, D-54501 Vandoeuvre-lès-Nancy, Nancy, France*

ABSTRACT

In the Livradois area of the French Massif Central, the Hercynian synorogenic porphyritic monzogranites and two-mica leucogranites intruded a migmatitic paragneiss sequence. Data on trace-element abundances and Rb/Sr and Sm/Nd isotopic values suggest a genetic link between the two-mica leucogranites and the migmatites. Numerical modeling of partial melting in the paragneiss can replicate the composition of the two-mica leucogranites in terms of trace elements if the accessory minerals zircon, monazite or xenotime remain in the residuum. The origin of the porphyritic monzogranite is more difficult to constrain; it belongs to a peculiar high-K, high-Mg suite that is rich both in compatible (*e.g.*, Mg) and incompatible (*e.g.*, K) elements. The porphyritic monzogranite is heterogeneous and contains microgranular mafic enclaves (MME) derived from a mafic magma. A model of mixing between a mafic magma with a composition similar to the MME, and a felsic magma similar to the two-mica leucogranite, accounts for the major- and trace-element characteristics and the Rb/Sr and Sm/Nd isotopic values of the porphyritic monzogranite. The MME are rich in incompatible elements, which implies an enriched source in the mantle. Considering the geological context of the Variscan belt in the French Massif Central, a possible origin for the enriched magmas is a subcontinental lithospheric mantle that was contaminated by crustal material during prior subduction, between 450 and 400 Ma. The results show that partial melting of a paragneiss generated the two-mica granite, and that the porphyritic monzogranite formed by mixing to various degrees of this melt with more mafic magmas generated by partial melting of an enriched mantle source. These magmas were formed and emplaced during the period 350 to 290 Ma when the orogen passed from the contractional (crustal thickening) stage to orogenic gravitational collapse after detachment of its eclogitic root.

*Keywords:* granite, magma, anatexis, mixing, high K-, high-Mg magma, mantle, Hercynian, French Massif Central.

<sup>§</sup> *E-mail address:* fabien\_solgadi@uqac.ca

## SOMMAIRE

La zone du Livradois, située dans le Massif Central français, comporte des intrusions synorogéniques de monzogranite porphyrique et de leucogranite à deux micas, mis en place dans une séquence de paragneiss migmatitiques. Les éléments traces ainsi que les rapports isotopiques Rb/Sr et Sm/Nd indiquent un lien génétique entre le leucogranite à deux micas et les migmatites. Les modèles numériques de fusion partielle du paragneiss aboutissent à des compositions similaires aux compositions du leucogranite à deux micas en termes d'éléments traces si les minéraux accessoires zircon, monazite ou xénotime restent dans les résidus de fusion. L'origine du monzogranite porphyrique est plus difficile à contraindre car il appartient à une suite particulière magnésio-potassique riche en éléments compatibles (*e.g.*, Mg) et incompatibles (*e.g.*, K). Le monzogranite porphyrique est hétérogène et contient des enclaves microgrenues sombres dérivant d'un magma mafique. Un modèle de mélange entre un magma mafique de composition similaire aux enclaves microgrenues sombres et un magma felsique de composition similaire au granite à deux micas montre des valeurs proches de celles du monzogranite porphyrique pour les éléments majeurs, les éléments traces et les rapports isotopiques Rb/Sr et Sm/Nd. Les enclaves microgrenues sombres sont riches en éléments incompatibles, ce qui implique une source mantellique enrichie. En considérant le contexte géologique du Massif Central, une possibilité pour obtenir un tel magma enrichi est de contaminer un manteau sous-continentale par un matériau crustal durant la période de subduction entre 450 et 400 Ma. Les résultats montrent que le leucogranite à deux micas provient de la fusion partielle du paragneiss, et que le monzogranite porphyrique s'est formé par le mélange de ce magma leucocratique avec un liquide issu de la fusion partielle d'un manteau enrichi. Ce magma s'est formé et s'est mis en place durant la période située entre 350 et 290 Ma, lorsque l'orogénèse passe du stade de contraction (épaississement crustal) au stade d'effondrement gravitaire après le détachement de sa racine éclogitique.

*Mots-clés:* granite, magma, anatexie, mélange, magma magnésio-potassique, manteau, Hercynien, Massif Central français.

## INTRODUCTION

Magmatism in zones of plate convergence displays various petrological and geochemical characteristics that reflect the source of the magma (*e.g.*, mantle *versus* crust) and the processes such as partial melting, fractional crystallization and magma mixing contributing to forming it (Bonin 1990, Chappell & White 1974, Peacock *et al.* 1994, Sawyer 1998, Thompson & Connolly 1995). Magmatic rocks typical of zones of active or past plate-convergence encompass: (1) calc-alkaline suites formed above the subducting plate, (2) peraluminous felsic suites resulting from anatexis of a thickened orogenic wedge, and (3) high-K, high-Mg magmatic rocks, exhibiting both mantle and crustal characteristics, the significance of which is much debated.

In this paper, we present some new petrological and geochemical data from the Livradois region in the core of the French Massif Central, where both peraluminous and high-K granitic rocks intrude a sequence of metasedimentary rocks that have been affected by anatexis. These data allow us to examine: (1) the genetic link between peraluminous leucogranite and the host anatectic paragneisses, (2) the relative contributions of mantle- and crust-derived magmas in the genesis of a high-K monzogranite, and (3) the impact of various processes such as partial melting, fractional crystallization, and magma mixing on the geochemical evolution of these magmas. The geodynamic significance of these results is discussed within the framework of the tectonic evolution of the Hercynian belt.

THE GEOLOGY OF THE HERCYNIAN BELT  
IN THE FRENCH MASSIF CENTRAL

The French Massif Central (Fig. 1) exposes a segment of the Hercynian middle crust characterized by large volumes of granite (*sensu lato*), migmatite, and metamorphic rocks (Dupraz & Didier 1988, Duthou *et al.* 1984, Pin & Peucat 1986). The Paleozoic tectonic evolution of this region was controlled by convergence between Gondwana and Laurasia that was accommodated by the subduction and accretion of crustal blocks (Franke 1989, Matte 1991, Pin & Duthou 1990). This evolution is recorded by the formation of an accretionary wedge that now comprises several nappes. This wedge was affected by metamorphism ranging from low to high geothermal gradients between the time of burial (420–350 Ma) and exhumation during gravitational collapse between 350 and 290 Ma (Burg *et al.* 1984, Pin & Peucat 1986, Vanderhaeghe *et al.* 1999). Ledru *et al.* (1989) recognized three major lithotectonic units (Fig. 1). From top to bottom, they are: (1) the Upper Gneiss Unit (UGU), (2) the Lower Gneiss Unit (LGU), and (3) the Para-autochthonous Unit, each of which now comprises a nappe. These nappes were partially melted, converted to migmatite, and then intruded by various plutonic rocks, ranging from a high-K suite to a peraluminous leucogranite suite, in the period between 350 and 290 Ma. The intrusion of plutonic rocks is considered to coincide with the transition from crustal thickening to crustal thinning in the area (Downes *et al.* 1990, Duthou *et al.* 1984, Pin & Duthou 1990). On the basis of their petrological and geochemical characteristics, these different plutonic suites are interpreted to involve crustal anatexis and the intrusion of mantle-derived magmas.

## GEOLOGY OF THE SOUTHERN LIVRADOIS AREA

The study area in the Livradois region is located in the core of the French Massif Central (Fig. 1). In this area, the local pile of nappes consists of: (1) the ophiolite-bearing Upper Gneiss Unit, which includes the so-called leptynite–amphibolite group at its base, and (2) the Lower Gneiss Unit (Burg *et al.* 1984, Ledru *et al.* 1989). The nappes underwent anatexis in the stability field of sillimanite, but contain relics of a higher-pressure metamorphism (Grange *et al.*, in prep.). The paragneisses of the Upper Gneiss Unit show a gradation from metatexite to diatexite migmatite from south to north (Fig. 1). The distinction between metatexite and diatexite is based on the proportion and disposition of the leucosome (Brown 1973, Mehnert 1968, Vanderhaeghe 2001). These rocks are characterized by a north-dipping, roughly east–west-trending penetrative foliation that has a northwest-trending stretching lineation. The composite nature of the foliation results from the alternation of leucosome and melanosome layers that is superimposed on a pre-existing, highly transposed compositional layering in the metasedimentary units. The foliation in the diatexite migmatite arises from the alignment of enclaves and schlieren. The foliation is concordant with the map-scale transition from metatexite to diatexite migmatites, although diatexite migmatite appears in the core of kilometer-scale domes and locally has discordant contacts with the foliation in the metatexite migmatite (Fig. 2). The migmatites are intruded by a number of veins of leucocratic granite that range from the centimeter to kilometer scale. In addition, a large sill of porphyritic monzogranite 10 km long and 2 to 3 km wide is intruded parallel to the foliation in the diatexite migmatite.

PETROLOGICAL DESCRIPTION  
OF MIGMATITES AND GRANITIC ROCKS  
OF THE SOUTHERN LIVRADOIS AREA

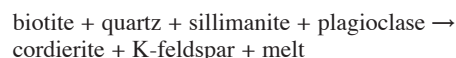
*Metatexite migmatites*

The metatexite migmatites are derived from psammitic and pelitic protoliths, and are characterized by a banding defined by the alternation of leucocratic and melanocratic layers. The average bulk modal composition of the metatexite migmatites is 30% quartz, 20% plagioclase (An<sub>20–26</sub>), 15% K-feldspar, 20% biotite, 5% muscovite, and 10% aluminosilicate minerals, cordierite, sillimanite and garnet. The accessory minerals monazite, xenotime, and zircon are ubiquitous, and commonly occur as inclusions in biotite.

The melanocratic part is fine-grained (0.5 to 1 mm) and comprises more than 80% of the rock. It is composed mainly of biotite, cordierite, sillimanite, and garnet. The leucocratic parts are medium-grained (1 to 2 mm), and occur principally as small lenses or layers. The modal composition of the leucocratic layers is

typically 40% quartz, 30% plagioclase (An<sub>0–7</sub>), 20% K-feldspar, 8% muscovite and 2% biotite and, thus, broadly leucogranodioritic. The leucocratic layers are interpreted to be derived from an anatectic melt, and their proportion in the paragneiss increases progressively toward the contacts with the intrusive granitic rocks.

The most common aluminous mineral in the metatexite migmatites is cordierite, but cordierite also contains some small crystals of sillimanite, suggesting the following reaction:



This reaction constrains the temperature of metamorphism to about 800°C, and indicates low to moderate pressures (between 2 and 7 kbar). Primary muscovite may have crystallized from the melt in place of K-feldspar during post-peak cooling, at temperatures of approximately 700°C (Storre & Karotke 1972).

*Diatexite migmatite*

Diatexite migmatite is a medium- to fine-grained rock (1 to 3 mm), with an overall modal mineral composition of 35% quartz, 25% plagioclase (An<sub>20–26</sub>), 10% K-feldspar, 15% biotite, 5% muscovite, and 10% aluminosilicate minerals, principally cordierite and rarely sillimanite. It has a very high proportion of leucosome, between 40 and 60% of the rock, and contains many centimeter-size lenses of melanosome, mostly composed of biotite and cordierite, oriented parallel to the general foliation. Enclaves of paragneiss (5 cm to 1 m) are common in the more leucocratic parts, and create a schollen diatexite (Mehnert 1968). The most common aluminous mineral is cordierite; because the mineral assemblages are similar to those in the metatexite migmatites, the diatexite is believed to have formed at similar metamorphic conditions.

*The two-mica leucogranite*

A kilometer-scale body of two-mica leucogranite (Figs. 3a, b) intruded the migmatites and pluton of porphyritic monzogranite. However, smaller bodies of two-mica leucogranite occur as segregations with diffuse borders in both the metatexite and diatexite migmatites; the segregations are generally oriented in the foliation plane. This two-mica leucogranite is believed to represent segregated anatectic melt derived from the migmatite developed at the expense of a pelitic assemblage. The two-mica leucogranite is fine-grained (1 to 2 mm), and contains 35% quartz, 30% plagioclase (An<sub>0–7</sub>), 20% K-feldspar, 5% biotite, and 10% primary muscovite; its overall composition is, therefore, “leucomonzogranite” in the Streckeisen (1976) classification. The accessory minerals, monazite and zircon, are rare.

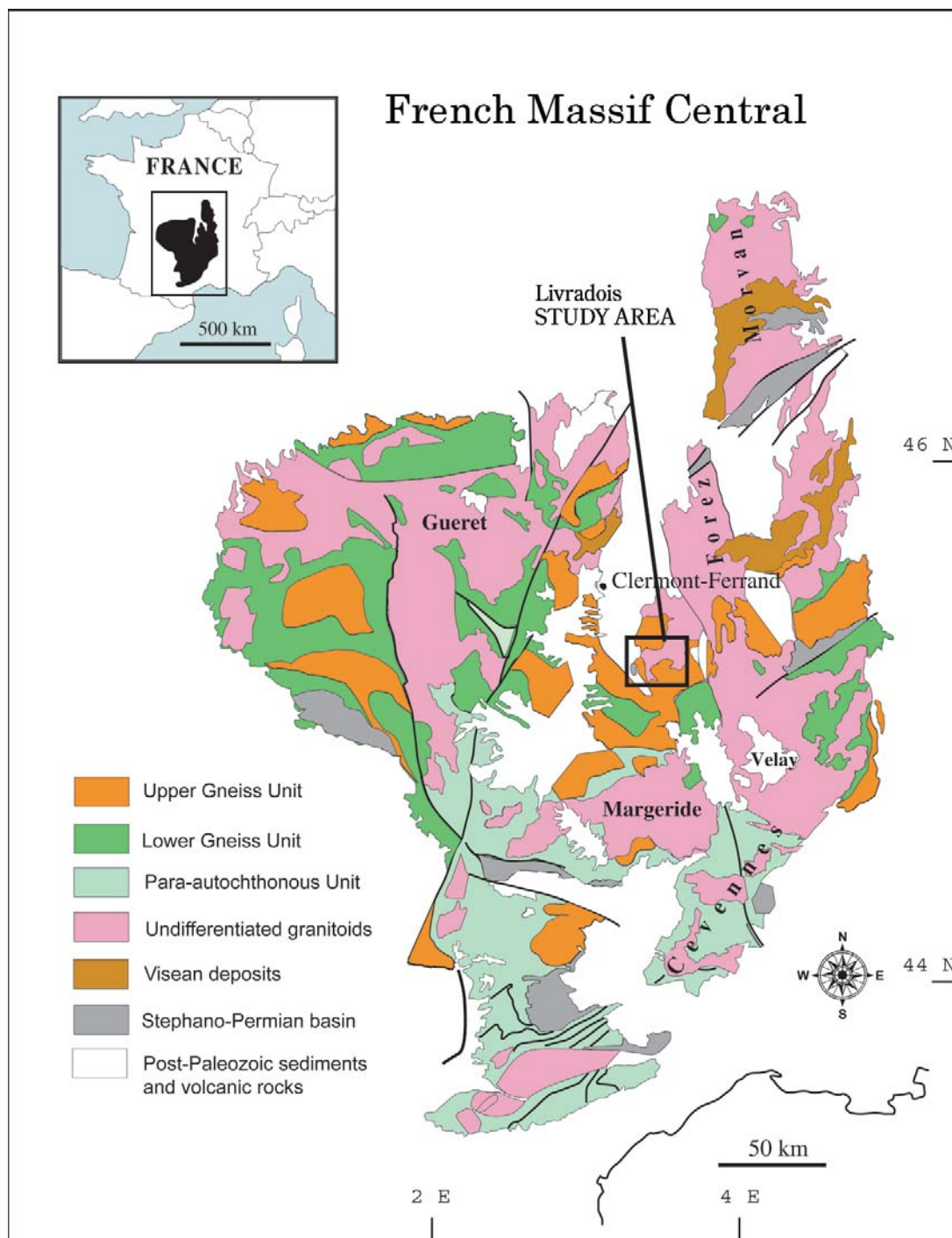


FIG. 1. Simplified geological map of the French Massif Central, modified from Ledru *et al.* (1989), with location of the study area.

A weak foliation due to the preferred orientation of mica is ubiquitous and oriented northeast, *i.e.*, parallel to the contacts. This fabric is believed to have been acquired in the magmatic state (Paterson *et al.* 1989) and is locally parallel to the foliation in the migmatites, particularly where the leucogranite occurs as intrusive sheets in the migmatites.

#### Porphyritic monzogranite

Porphyritic monzogranite forms a large (8 × 4 km) sill in the migmatites. It is a coarse-grained rock (2–3 mm) containing poikilitic K-feldspar megacrysts 1–3 cm across that have inclusions of biotite, quartz and plagioclase. The bulk rock contains 30% quartz, 30% plagioclase (*ca.* An<sub>30</sub>), 30% K-feldspar (mostly as megacrysts) and 10% biotite. The accessory minerals zircon, apatite and allanite are common. The K-feldspar megacrysts and biotite define a weak foliation in the center of the porphyritic monzogranite, and because the minerals display little internal deformation, this fabric is inferred to be magmatic in origin (Paterson *et al.* 1989). Quartz-filled fractures are present in some of the plagioclase crystals (Fig. 3a) and indicate that deformation of the crystal framework occurred while

some residual melt remained (Bouchez *et al.* 1992). The local development of recrystallized ribbons of quartz indicates some subsolidus deformation of the porphyritic monzogranite (Paterson *et al.* 1989, Vernon *et al.* 1983). In contrast, the southern border of the intrusion is mylonitic, indicating intensive subsolidus deformation there (Fig. 2). These features, taken together, point to a syntectonic emplacement for this sill.

The porphyritic monzogranite is heterogeneous at the outcrop scale (Fig. 4a), and comprises: (1) foliation-parallel, meter-sized layers rich in K-feldspar crystals, (2) zones concordant to the foliation that are devoid of K-feldspar megacrysts and, (3) veins of biotite-bearing leucogranite (20–50 cm wide) that have a diffuse border and are discordant to the foliation in the porphyritic monzogranite. Collectively, these features are thought to indicate the segregation of the melt fraction during crystallization. The megacryst-free layers and the veins represent the residual melt extracted from the regions now marked by the zones rich in K-feldspar. The accumulation of K-feldspar may have occurred by crowding of crystals (Vernon 1986) during magmatic flow. The porphyritic monzogranite contains elongate mm-scale xenoliths of muscovite-rich paragneiss. Myrmekite is developed at the edges of the paragneiss xenoliths

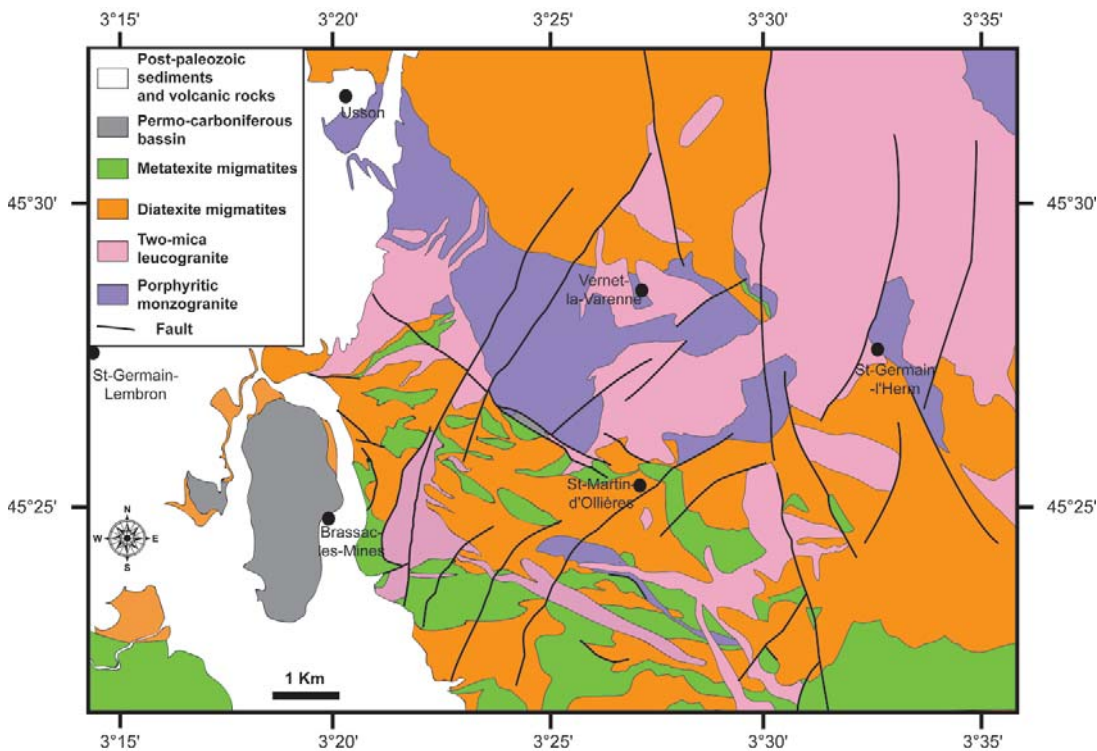


FIG. 2. Geological map of the study area showing the relationship between the different rock-types.

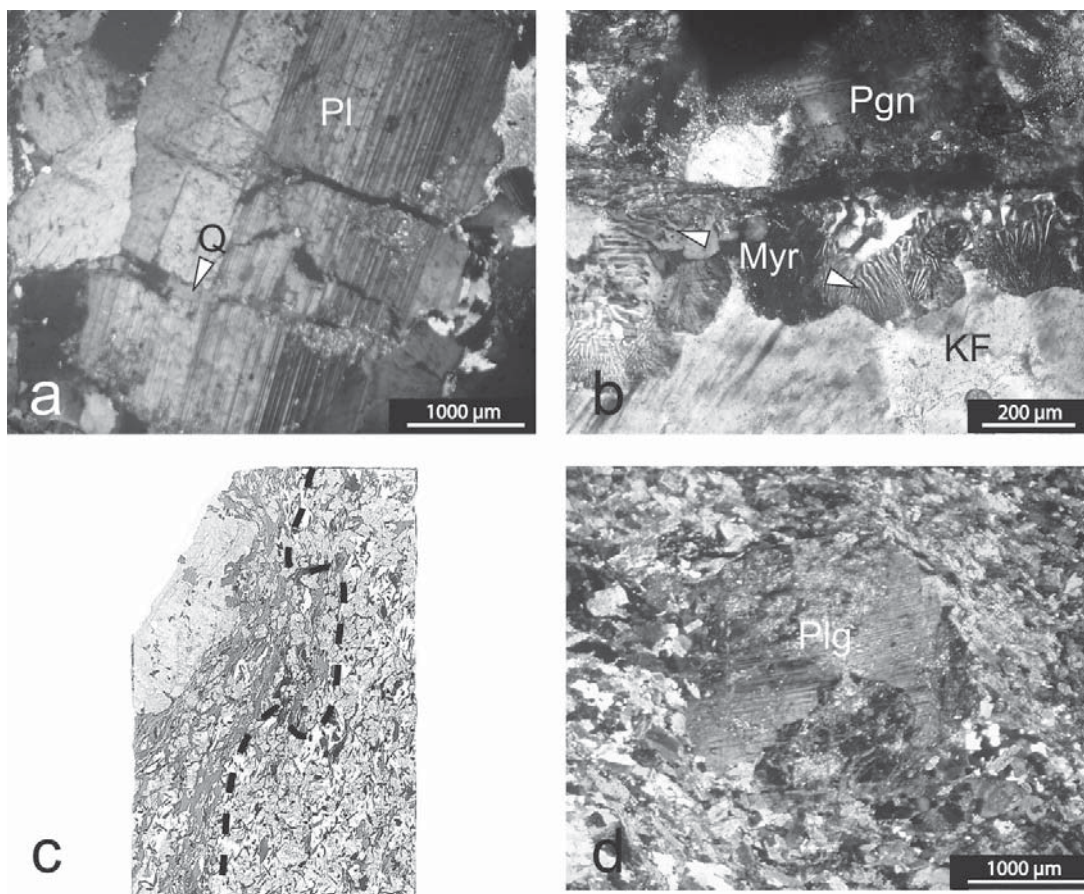


FIG. 3. Photomicrographs of thin sections to illustrate (a) Plagioclase (Plg) with fractures, from porphyritic monzogranite; the fractures are filled by quartz (Q). (b) Myrmekitic structure (Myr) created by the chemical destabilization of K-feldspar (KF) next to the paragneiss (Pgn). (c) Entire thin sections  $\times \sim 24$  by 35 mm showing the edge of an MME. Note the larger crystals of biotite at the border. (d) Rounded plagioclase (Plg) in an MME.

(Fig. 3b), and indicates chemical disequilibrium with the host monzogranite.

There are two types of plagioclase in the porphyritic monzogranite:

1) Plagioclase with a simple pattern of zoning (Fig. 5a) in which the An content gradually decreases from core ( $An_{30}$ ) to rim ( $An_{20}$ ). This normal zoning records the evolution of the magma's composition during fractional crystallization (Wiebe 1968).

2) Plagioclase with a complex core (Fig. 5b), containing some irregularly shaped calcic ( $An_{40}$ ) regions interspersed with less calcic ( $An_{30}$ ) regions, that are surrounded by an even less calcic rim. Plagioclase with complex cores have been regarded as indicative of hybrid magmas (Castro 2001, Vernon 1984). First, a moderately calcic ( $An_{30}$ ) plagioclase crystallized from a felsic magma, then a high-temperature, more mafic

magma was intruded and caused resorption of the plagioclase, and then new, more calcic ( $An_{40}$ ) plagioclase grew around the resorbed plagioclase relic. During subsequent crystallization, the complex plagioclase acts as a nucleus for the crystallization of Ca-poor plagioclase that crystallizes from the hybrid magma (Fig. 6).

#### *Mafic microgranular enclaves*

Mafic microgranular enclaves (MME) are common in the porphyritic monzogranite (Barbarin 1988, Didier & Barbarin 1991). The enclaves are 5–20 cm long (Fig. 4b), and elongate in the foliation, consistent with deformation under magmatic conditions (Wiebe & Collins 1998). Typically, the MME are fine-grained (0.2 to 1 mm) and consist of 15% quartz, 30% plagioclase ( $An_{30}$ ), 15% K-feldspar and 40% biotite and, rarely,

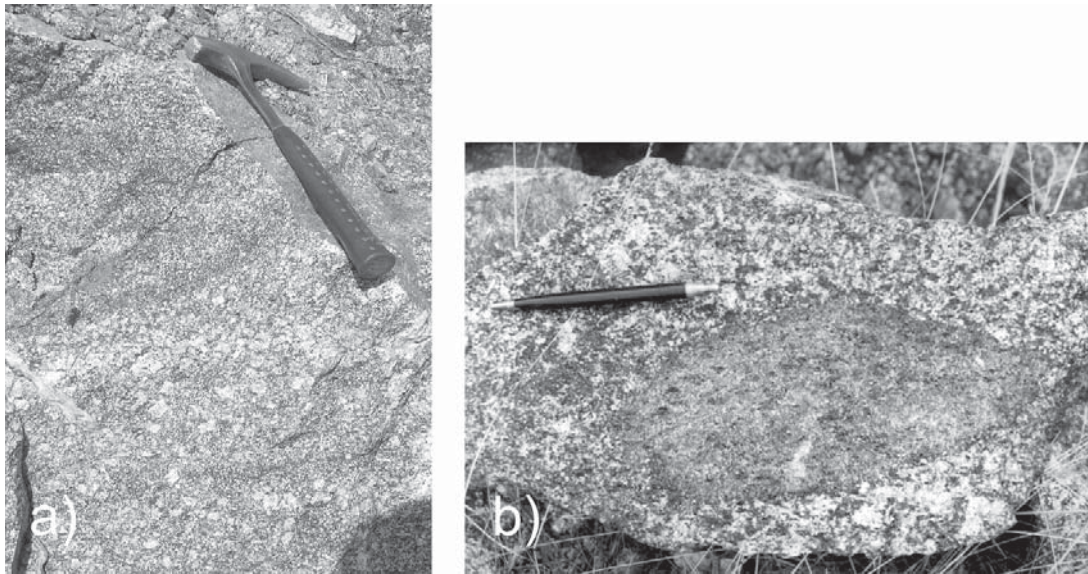


FIG. 4. (a) Field photographs from the porphyritic monzogranite NW showing heterogeneity, with accumulation of K-feldspar in layers. (b) Microgranular mafic enclave (MME) in porphyritic monzogranite. Pen is 15 cm long.

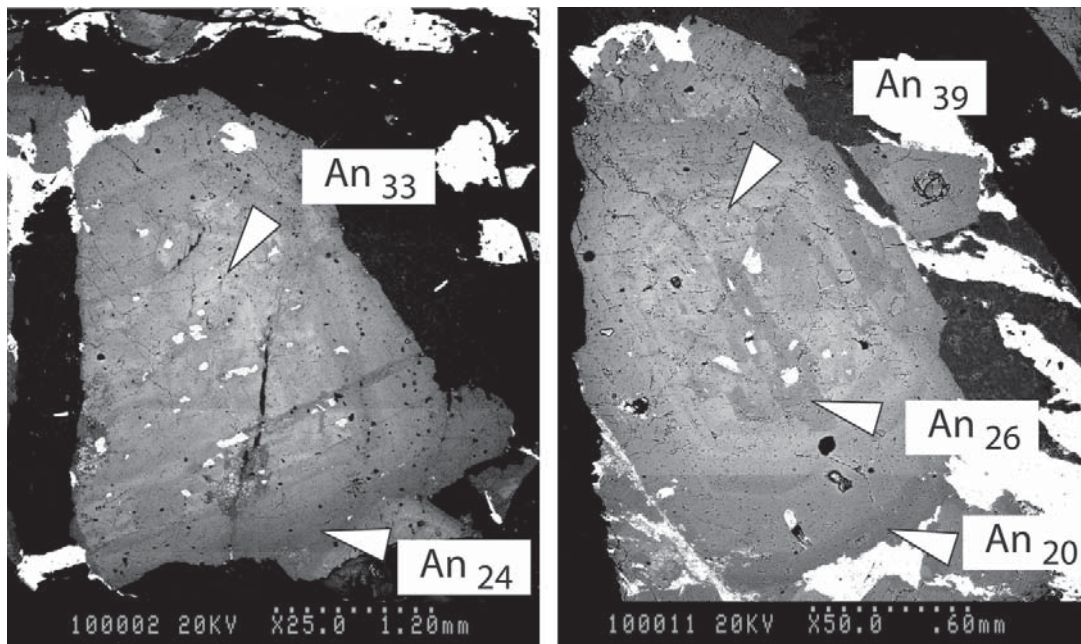


FIG. 5. Back-scattered-electron (BSE) images (Z contrast) of plagioclase from a porphyritic monzogranite. (a) Plagioclase with simple zonation created by fractional crystallization. (b) Plagioclase with complex zoning (see Fig. 6).

amphibole. Zircon and apatite are common accessory minerals. The grain size of biotite in the MME varies from <1 mm in the core, to >1 mm at the rim, where it is (Fig. 3c) comparable in size to biotite in the host porphyritic monzogranite. The biotite in the monzogranite host thus seems to have been mechanically assembled around the enclave, forming a dark rim (Fig. 3c). Large (2 mm) crystals of allanite occur in the rim zone of MME and are stabilized by the high

Ca content and low  $[Al/(Ca + Na + K)]$  of the MME (Cuney & Friedrich 1987). The stability of the allanite in such material is commonly interpreted as evidence for hybridation (Dini *et al.* 2004). Rounded K-feldspar phenocrysts (Fig. 3d) that are macroscopically similar to the K-feldspar megacrysts in the porphyritic monzogranite occur in the MME. Such a relationship is commonly interpreted to result from the chemical destabilization, and subsequent corrosion, of feldspar

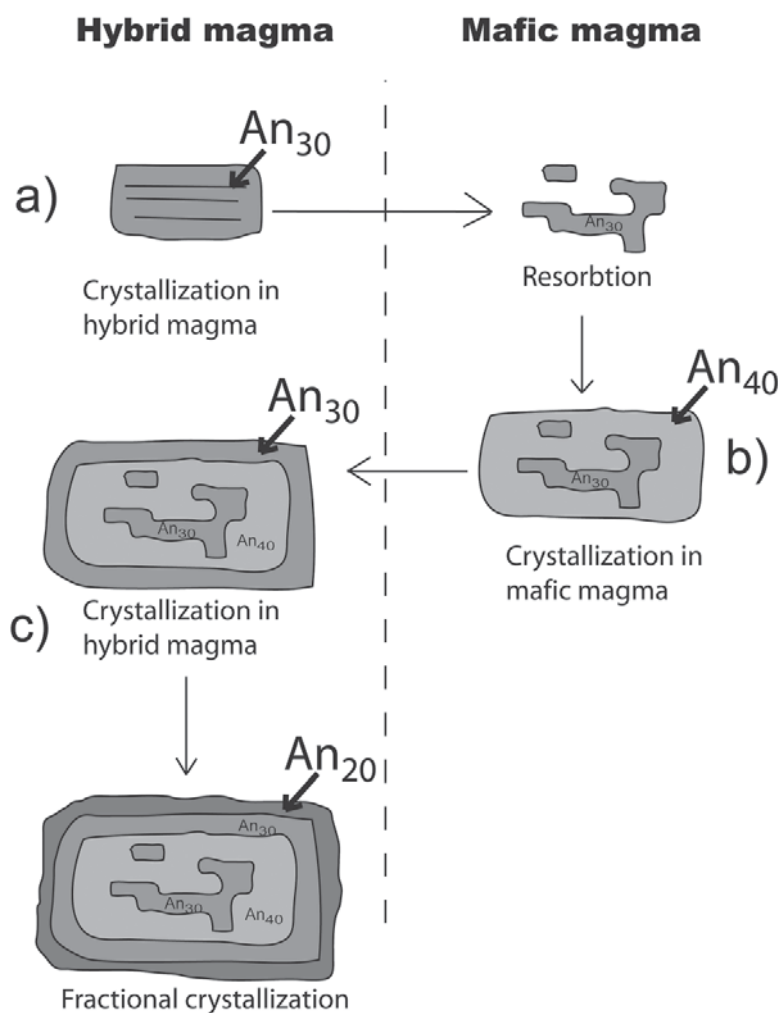


FIG. 6. Formation of plagioclase with complex core-structure in porphyritic monzogranite by mixing of a mafic magma with a felsic one (*e.g.*, Castro 2001). (a) When plagioclase that crystallized from the hybrid magma comes to contact with a mafic magma, the plagioclase is resorbed. (b) A calcic plagioclase ( $An_{40}$ ) crystallizes in the mafic magma around the resorbed plagioclase. (c) The plagioclase now has a complex core-structure. New plagioclase of composition  $An_{30}$  crystallizes from the hybrid magma. By the process of fractional crystallization, later growth of plagioclase is progressively less calcic, down to  $An_{20}$ .

megacrysts that crystallized in the felsic porphyritic monzogranite and were incorporated into the mafic magma from which the enclave formed (Barbarin 1988, Pin *et al.* 1990, Pin & Duthou 1990).

## GEOCHEMISTRY

### *Analytical methods*

Thirty-four samples were selected for the determination of major- and trace-element contents. The whole-rock determinations were made at the SARM (Service d'Analyse des Roches et des Minéraux), CNRS-CRPG Vandoeuvre, France, using inductively coupled plasma – atomic emission spectroscopy (ICP–AES) for major elements and inductively coupled plasma – mass spectrometry (ICP–MS) for trace elements. The precision is estimated to be better than 2% for values higher than 5 wt% for the major oxides, and better than 15% in the range of 1 to 10 ppm for the trace elements. The results are given in Table 1.

The Rb–Sr and Nd–Sm isotopic compositions were determined for twelve samples. Approximately 100 mg of sample powder were spiked with isotopic tracers and dissolved in a concentrated HF–HNO<sub>3</sub>–HClO<sub>4</sub> acid mixture, and heated (110°C) for at least 72 hours in a closed teflon beaker. Both Rb and Sr were separated by conventional cation-exchange techniques using AGX 50W resin with 2.5 N HCl acid. After rinsing with 2.9 N HNO<sub>3</sub>, the rare-earth elements (REE) were extracted from the same cation-exchange columns with 4.4 N HNO<sub>3</sub>; Nd and Sm were subsequently isolated from the other REE using HDEHP-coated teflon resin columns with 0.27 N and 0.5 N HCl, respectively.

The isotopic composition of Rb was determined at the SARM using an ELAN 6000 ICP–MS instrument. The isotopic compositions of Sr, Nd and Sm were determined in static multicollecion mode using a Finnigan MAT 262 mass spectrometer at CNRS-CRPG Vandoeuvre. Concentrations were calculated by isotope dilution. The Sr samples were loaded on single W filaments, but Sm and Nd were loaded on Ta filaments and ionized using a Re filament. Measured <sup>87</sup>Sr/<sup>86</sup>Sr values were normalized to <sup>86</sup>Sr/<sup>88</sup>Sr = 0.1194. The Nd isotope ratios were normalized to <sup>146</sup>Nd/<sup>144</sup>Nd = 0.7219. During the period of analysis, our value for the La Jolla Nd standard was 0.511799 ± 0.000022 (2σ), whereas the value for the NBS987 Sr standard was 0.710166 ± 0.000048 (2σ). These values differ significantly from the generally accepted values for these standards (La Jolla: 0.511854; NBS987: 0.71024), most probably due to aging of the Faraday cups. Nevertheless, determinations of other standards during the same time period showed equivalent shifts, demonstrating that the shift is insensitive to isotopic composition. All the results presented in Table 2 have been corrected by the amounts needed to bring the La Jolla and NBS987 standards into agreement with their internationally accepted values.

Total chemical blanks were <2 ng for Sr and ~0.4 ng for Nd, and thus have no significant effect on the isotopic compositions.

Initial ratios and ε<sub>Nd</sub> have been calculated at 300 My (estimated age from geological relationships). The maximum uncertainty in the age is ±20 My, but this has only a minor effect on the calculated initial ratio (ε<sub>Nd</sub> changes by a maximum of 0.3 units). Small but systematic differences are observed between the Sm concentrations obtained by ICP–MS (after fusion with LiBO<sub>4</sub>) and those obtained by isotope dilution after acid digestion, especially for the leucogranites. The differences probably reflect a failure to completely dissolve zircon during acid digestion. Nevertheless, in most cases, the Sm/Nd ratio obtained by the two methods agree within 10%, and the difference is only 24% in the worst case (sample 8). In any event, assuming that the samples were in isotopic equilibrium at 300 My, this should have no effect on the calculated initial ratios.

### *Interpretation of paragneiss and leucogranite*

The migmatitic paragneiss has a A/CNK value between 1.30 and 2.45 and is peraluminous, consistent with a metasedimentary protolith, but it is also rich in Fe (~6 wt% Fe<sub>2</sub>O<sub>3</sub>). The two-mica leucogranite also is peraluminous (A/CNK values between 1.2 and 1.5), but it contains less than 2 wt% Fe<sub>2</sub>O<sub>3</sub> (Table 1). Harker diagrams (Fig. 7) for the anatectic metasedimentary rocks (*i.e.*, metatexite migmatite, diatexite migmatite and enclaves of paragneiss) show a negative correlation for SiO<sub>2</sub> with Al<sub>2</sub>O<sub>3</sub> and with Fe<sub>2</sub>O<sub>3T</sub>. This trend probably reflects variations in the mixing ratio between two end-member compositions of sediment, one a clay-dominated pelite (Al- and Fe-rich, Si-poor), and the other a (quartz + feldspar)-dominated psammite (greywacke). Harker diagrams (Figs. 7c, d) show positive correlations for Ca and Na with SiO<sub>2</sub>. Plagioclase is the principal Ca- and Na-bearing mineral in these rocks. This positive correlation can be explained by progressively higher proportion of plagioclase in the more siliceous metasedimentary rocks.

Figure 8 shows that the migmatitic paragneisses have relatively high concentrations of the REE (*e.g.*, La 48 to 77 ppm) compared with the two-mica leucogranite (La 2.3 and 26 ppm). Table 1 shows that the two-mica leucogranites have a much greater range in REE contents than the migmatites. However, relative to the REE, the two-mica granites are depleted in Th and Zr compared to the metasedimentary migmatites.

The Rb/Sr and Sm/Nd isotopic ratios of four samples of leucogranite and three of the migmatites (two metatexite and one diatexite) were determined with the objective of constraining the origin of the two-mica leucogranite, and to test a potential genetic link to the migmatitic paragneiss. The Sr and Nd isotope compositions were recalculated to 300 My, the probable age of granite emplacement in this region (Ledru *et*

TABLE 1. CHEMICAL COMPOSITION OF ROCKS OF THE LIVRADOIS SUITE, FRENCH MASSIF CENTRAL

sample number	Two-mica leucogranite																
	SGL	SGL	SGL	SGL	SGL	SGL	SGE					SGL	SGL	SGL			
	2K	2K	2K	2K	2K	2K	01	F161	32B	36	F132	F165B	2K	2K	2K		
8	28	19	14	3a	152	25a	54	F161	32B	36	F132	F165B	12	20b	23a	89	
SiO <sub>2</sub>	72.25	70.17	71.31	71.68	72.15	72.69	73.53	70.71	74.93	74.60	75.31	74.75	74.04	75.32	74.74	74.79	76.52
TiO <sub>2</sub>	0.23	0.29	0.24	0.22	0.15	0.17	0.12	0.31	b.d.l.	0.03	b.d.l.	b.d.l.	0.12	0.11	0.09	b.d.l.	0.05
Al <sub>2</sub> O <sub>3</sub>	15.37	15.74	15.7	15.54	15.29	15.27	14.85	15.39	14.35	14.57	14.11	14.47	14.4	13.76	14.92	14.07	13.81
Fe <sub>2</sub> O <sub>3t</sub>	1.30	2.38	1.93	1.69	0.88	1.17	1.3	2.15	0.81	0.71	0.79	0.73	1.09	1.07	1.11	0.94	0.48
MnO	b.d.l.	b.d.l.	b.d.l.	b.d.l.	b.d.l.	b.d.l.	b.d.l.	0.03	b.d.l.	0.02	b.d.l.						
MgO	0.32	0.78	0.59	0.51	0.27	0.19	0.27	0.81	0.16	0.16	0.13	0.1	0.25	0.14	0.2	0.12	0.11
CaO	0.39	1.25	0.53	0.5	0.76	0.48	0.84	1.56	0.47	0.44	0.35	0.48	0.62	0.2	0.61	0.29	0.14
Na <sub>2</sub> O	3.20	3.49	3.5	3.57	3.63	3.42	3.48	3.39	3.74	3.48	3.39	3.62	3.15	3.59	2.15	3.45	3.05
K <sub>2</sub> O	4.54	3.47	4.13	4.19	5.29	4.68	4.15	4.15	4.1	3.96	4.24	4.38	4.92	4.13	4.56	4.89	4.00
P <sub>2</sub> O <sub>5</sub>	0.14	0.13	0.19	0.16	0.17	0.14	0.13	0.14	0.1	0.24	0.20	0.17	0.18	0.15	0.12	0.13	0.09
LOI	2.08	2.15	1.8	1.74	0.76	1.60	1.19	1.12	1.09	1.54	1.20	1.02	1.0	1.28	1.49	0.92	1.52
Total	99.82	99.85	99.92	99.80	99.35	99.81	99.86	99.76	99.75	99.75	99.72	99.72	99.77	99.75	99.99	99.60	99.77
Cr	8.86	13.25	17.36	14.8	12.48	9.71	11.18	11.36	5.31	b.d.l.	b.d.l.	b.d.l.	6.59	9.187	12.15	5.576	b.d.l.
Ni	0.00	8.29	7.793	6.538	b.d.l.	5.10	7.558	5.27	b.d.l.	0.00	0.00	b.d.l.	b.d.l.	b.d.l.	5.93	b.d.l.	0.00
Co	1.13	4.155	2.254	1.882	0.997	1.07	2.147	3.273	0.553	0.46	0.43	0.632	1.661	0.93	1.624	1.207	0.38
V	13.58	25.14	19.65	16.64	11.25	9.30	9.006	24.68	2.759	b.d.l.	2.80	2.287	7.475	9.858	8.265	1.833	5.31
Ga	25.96	23.34	24.5	26.21	20.99	21.76	21.33	23.06	17.96	18.55	17.09	15.47	14.55	15.11	17.99	18.52	14.66
Cs	7.11	16.98	6.014	6.228	9.174	15.22	6.511	7.512	3.062	19.45	13.26	6.31	4.375	4.524	2.187	5.625	5.21
Rb	210.10	119.4	190.6	168.9	165.1	206.24	140.4	162.4	206.24	249.00	203.85	154.9	146.3	164.6	111.4	189.7	187.34
Ba	408.25	912.4	473.5	432.8	348.6	465.87	621.7	758.2	465.87	81.14	108.08	114	314	553.5	428.6	391.1	222.04
Th	8.56	10.37	9.957	10.11	5.588	7.79	6.585	12.11	7.79	0.65	1.04	1.427	3.068	4.767	6.158	5.07	1.39
U	4.61	2.997	4.055	4.249	4.041	2.93	4.439	5.16	2.93	2.73	4.34	2.512	4.163	5.803	3.962	2.727	1.87
Ta	1.08	1.365	1.178	1.231	1.742	1.40	1.137	1.162	0.87	2.99	1.49	1.229	0.959	1.778	0.835	1.506	1.72
Nb	7.28	8.195	7.387	6.848	7.545	8.13	6.347	8.273	8.13	8.66	7.79	6.271	4.702	7.077	5.832	7.079	6.96
Sr	100.41	304.9	137.8	135.3	144.1	128.20	171.3	313.3	128.19	28.30	44.33	68.47	119.6	119.7	103.2	70.23	43.04
Hf	2.98	3.595	3.142	3.185	1.929	2.37	2.17	3.811	1.45	1.07	1.12	0.98	1.325	1.922	1.894	1.583	1.07
Zr	93.29	112.1	98.41	100.5	53.9	74.49	56.97	122.5	74.49	20.99	28.19	25.24	39.94	57.02	47.47	35.43	28.75
Y	9.84	18.27	11.41	10.47	8.685	12.73	16.65	13.08	13.75	6.11	7.91	11.72	12.22	16.99	16.65	15.24	9.36
La	20.70	26.64	22.89	21.17	11.38	18.08	14.35	29.21	10.02	2.30	3.21	4.495	7.23	11.76	12.92	7.792	4.86
Ce	41.95	54.99	47.74	45.44	23.79	33.93	30.33	59.19	21.73	4.20	6.55	9.019	14.84	24.78	27.86	17.16	8.72
Pr	5.20	6.53	5.719	5.446	2.82	4.26	3.676	6.994	2.512	0.61	0.84	1.135	1.768	2.976	3.33	2.116	1.09
Nd	18.82	23.77	20.7	19.72	10.16	15.88	13.53	25.66	9.175	2.19	3.08	4.001	6.474	10.96	12.49	7.613	3.95
Sm	4.06	4.592	4.321	4.123	2.104	3.35	3.157	4.783	2.403	0.68	0.74	1.213	1.559	2.512	2.974	2.268	0.83
Eu	0.61	1.105	0.747	0.61	0.6	0.81	0.678	0.948	0.486	0.18	0.19	0.29	0.568	0.554	0.548	0.303	0.18
Gd	2.85	3.7	3.185	2.887	1.594	2.66	2.845	3.537	2.404	0.75	0.86	1.337	1.628	2.459	2.968	2.229	0.88
Tb	0.42	0.592	0.444	0.402	0.268	0.40	0.502	0.501	0.411	0.16	0.18	0.281	0.293	0.438	0.495	0.44	0.18
Dy	2.04	3.318	2.358	2.081	1.542	2.29	3.004	2.526	2.34	1.20	1.27	1.959	2.004	2.872	2.957	2.597	1.31
Ho	0.33	0.609	0.383	0.351	0.288	0.42	0.555	0.459	0.405	0.19	0.26	0.375	0.395	0.555	0.548	0.475	0.29
Er	0.85	1.689	1.003	0.921	0.824	1.07	1.525	1.192	1.081	0.57	0.73	1.086	1.221	1.538	1.517	1.311	0.87
Tm	0.11	0.253	0.145	0.138	0.126	0.17	0.237	0.165	0.157	0.09	0.15	0.187	0.196	0.22	0.221	0.195	0.17
Yb	0.63	1.718	0.957	0.913	0.913	1.10	1.625	1.142	0.967	0.74	1.09	1.372	1.384	1.424	1.48	1.319	1.15
Lu	0.09	0.25	0.133	0.136	0.138	0.15	0.243	0.164	0.135	0.10	0.17	0.201	0.21	0.204	0.214	0.186	0.16

*al.* 1989). The migmatites have an  $\epsilon\text{Nd}$  value between  $-8.36$  and  $-7.46$  and a  $^{87}\text{Sr}/^{86}\text{Sr}$  ratio between  $0.713610$  and  $0.715471$ ; these are similar to the values obtained from the two-mica leucogranite,  $\epsilon\text{Nd}$  between  $-9.31$  and

$-7.10$  and a  $^{87}\text{Sr}/^{86}\text{Sr}$  between  $0.716355$  and  $0.718193$ . Therefore, two-mica leucogranite has isotopic ratios that are consistent with an origin by partial melting of the paragneiss at about  $300$  Ma (Fig. 9).

TABLE 1 (cont'd). CHEMICAL COMPOSITION OF ROCKS OF THE LIVRADOIS SUITE, FRENCH MASSIF CENTRAL

sample number	Porphyritic monzogranite			MME		Diatexite					Paragneiss				
	155B	155E	SGW79 D	SGW79 155C	SGE01 C	SGE01 -16	SGE01 -191a	SGE01 -25	SGE01 -117	F84	F 82A	SGE01 -157	SGL2K 24	SGE01 -187	SGE01 -24
SiO <sub>2</sub>	63.43	66.17	69.82	62.68	53.91	64.75	70.74	64.31	60.93	67.54	70.63	69.3	66.69	65.74	65.61
TiO <sub>2</sub>	0.63	0.57	0.41	0.93	0.76	0.85	0.68	0.68	1.13	0.54	0.24	0.74	0.73	0.74	0.88
Al <sub>2</sub> O <sub>3</sub>	15.69	15.46	14.84	14.23	15.7	16.66	14.28	16.66	17.99	15.83	15.67	14.62	15.93	16.09	16.36
Fe <sub>2</sub> O <sub>3t</sub>	4.51	4.01	3.02	6.31	8.83	6.54	4.57	4.6	8.34	4.57	2.04	5.39	5.76	6.06	7.23
MnO	0.06	0.05	0.05	0.09	0.14	0.06	0.04	0.06	0.11	0.04	b.d.l.	0.08	0.04	0.04	0.09
MgO	2.81	2.08	1.77	3.92	6.25	2.04	1.45	2.23	2.02	1.71	0.64	1.64	2.03	2.3	2.86
CaO	2.66	2.41	2.05	3.09	4.19	1.05	1.33	1.23	0.85	1.1	0.69	2.0	0.43	0.4	1.02
Na <sub>2</sub> O	2.88	3.11	3.01	2.71	3.03	1.91	2.46	3.54	1.99	2.59	3.21	2.3	1.97	1.48	1.45
K <sub>2</sub> O	4.79	4.53	4.24	3.63	2.35	3.45	2.7	4.42	5.07	3.85	4.66	2.3	3.69	3.33	3.29
P <sub>2</sub> O <sub>5</sub>	0.30	0.15	0.08	0.41	0.5	0.14	0.09	0.33	0.12	0.21	0.16	0.1	0.11	0.11	0.16
LOI	2.18	1.36	0.97	1.93	4.63	2.86	1.52	1.61	1.43	1.88	1.88	0.96	2.69	3.59	1.15
Total	99.94	99.90	100.26	99.93	100.29	100.31	99.86	99.67	99.98	99.86	99.82	99.43	100.07	99.88	100.10
Cr	110.02	68.19	68.47	203.40	637.2	93.22	61.97	57.28	124.4	61.86	21.33	77.88	86.89	90.62	118.4
Ni	35.36	27.64	24.91	55.46	191	39.12	26.58	17.36	47.2	45.74	7.012	24.42	26.16	38.41	49.71
Co	12.40	11.73	9.898	17.52	27.35	11.55	10.24	11.2	20.58	11.98	2.877	13.67	11.35	10.03	20.24
V	66.49	67.76	63.51	88.73	144.6	121.5	73.34	71.28	134.4	71.04	24.07	108.5	101.8	118.1	160
Ga	23.55	22.02	21.75	25.40	29.41	23.84	19.22	25.81	28.68	22.26	20.95	26.74	26.57	23.05	26.14
Cs	12.35	9.65	9.729	14.40	15.6	8.296	4.184	10.79	9.35	13.81	9.765	1.706	10.36	12.33	4.088
Rb	218.79	195.90	179.5	243.25	193.6	146.8	94.76	200.1	226.8	167.9	177.1	104.8	163.4	146.5	145.5
Ba	981.51	807.91	968.6	682.43	120.3	804	612	1099	1386	637.1	593.6	504.4	1199	594.5	930.7
Th	31.01	51.57	30.69	30.22	50.13	16.59	15.18	14.1	26.24	14.12	13.85	31.08	26.44	15.41	16.78
U	11.06	17.90	10.29	8.04	11.2	2.579	4.412	3.22	4.92	5.167	4.362	2.882	7.373	4.304	3.429
Ta	2.08	2.12	1.652	1.86	2.408	1.007	0.741	1.597	2.122	1.414	1.177	2.173	1.114	1.032	1.246
Nb	18.68	15.87	13.15	24.25	22.6	13.95	10.55	14.86	23	10.98	7.772	18.6	15.01	11.83	13.56
Sr	391.58	339.97	400.1	306.10	366.1	157.4	182.1	296.9	264.4	177.1	161.7	201.3	192.4	134.3	175.3
Hf	7.15	7.26	7.569	10.52	10.06	6.816	7.922	6.022	10.97	5.863	3.858	12.67	9.647	6.43	7.519
Zr	254.34	240.76	245.4	376.72	340.5	241.8	287.5	221.7	408.2	207.5	125.1	468.7	359.6	236.6	270.7
Y	20.81	10.72	6.636	28.22	60.56	34.39	24.64	24.35	40.56	25.37	19.97	38.75	25.59	35.85	40.01
La	47.83	52.91	8.962	64.98	46.15	47.68	45.76	38.56	77.86	36.89	27.67	77.54	68.9	48.06	51.16
Ce	96.10	112.74	18.34	131.81	107.5	96.42	87.05	76.78	154.8	75.03	59.18	150.8	135.3	94.46	105
Pr	11.75	13.60	2.216	15.64	15.84	11.19	10.19	9.057	17.51	8.775	6.704	17.45	15.37	11.23	12.44
Nd	42.65	50.11	8.855	60.54	72.49	42.56	37.61	34.96	64.5	32.49	24.52	64.6	56.02	41.56	46.72
Sm	8.03	7.46	1.83	10.50	18.92	8.227	6.861	6.938	11.62	6.519	5.022	11.23	10.26	8.373	9.293
Eu	1.60	1.51	1.505	1.13	1.62	1.445	1.566	1.423	1.875	1.25	0.795	1.717	1.726	1.389	1.764
Gd	5.79	3.49	1.401	7.40	14.71	6.918	5.618	5.59	9.081	5.226	3.893	7.836	7.977	6.799	8.012
Tb	0.81	0.51	0.209	1.07	2.145	1.064	0.839	0.872	1.388	0.839	0.598	1.175	1.019	1.085	1.257
Dy	4.18	2.48	1.132	5.51	11.85	6.246	4.633	4.921	7.788	4.889	3.631	6.758	5.372	6.433	7.251
Ho	0.70	0.39	0.227	0.97	2.101	1.241	0.884	0.919	1.419	0.906	0.65	1.346	0.918	1.252	1.451
Er	2.02	1.10	0.676	2.59	5.702	3.529	2.442	2.19	4.033	2.483	1.868	4.084	2.398	3.508	3.994
Tm	0.25	0.18	0.118	0.35	0.843	0.564	0.37	0.242	0.593	0.374	0.279	0.635	0.337	0.492	0.61
Yb	1.90	1.25	0.909	2.29	5.187	3.785	2.437	1.315	3.94	2.575	1.918	4.341	2.261	3.314	4.161
Lu	0.26	0.24	0.167	0.28	0.734	0.592	0.376	0.195	0.611	0.397	0.279	0.664	0.354	0.509	0.648

b.d.l.: below detection limit. The major-element are reported in wt%, and the trace elements, in ppm. MME: microgranular mafic enclave.

### Geological modeling of the two-mica leucogranite

The two-mica leucogranite can be modeled as a partial melt of a pelitic metasedimentary protolith, using

an equation to describe equilibrium partial melting (Allègre & Minster 1978, Shaw 1970). A simple model with a biotite-rich residuum, and modal proportions similar to those observed in the enclaves of residual

paragneiss from the diatexite migmatite (Fig. 10a), do not account for the trace-element composition of the leucogranites. In particular, the predicted REE contents for the model melt are too high compared to the values obtained from the two-mica leucogranite. The REE have low partition-coefficients into the major phases; the minor phases that have high partition-coefficients for the REE (zircon, monazite, xenotime or apatite) thus remained in the residuum, as has been reported previously for leucogranites and S-type granites (Montel 1993). Adding 1% of zircon to the model restite causes a large increase in the bulk  $D$  values for REE (*e.g.*,

from 0.4 to 5.6 for  $D_{Yb}$ ), and results in melt compositions that are in good agreement with the natural leucogranites (Fig. 10b). Although 1% zircon is far too great an amount compared to that present in the paragneiss enclaves, it serves to illustrate what effect a large proportion of accessory phases in the residuum would have, monazite and xenotime for example, for which the partition coefficients for REE are even greater than for zircon (Bea *et al.* 1994, 2006). The large range in REE composition of the two-mica leucogranite may well be related, therefore, to whether the accessory phases remained in the residuum during anatexis or not.

TABLE 2. Sm–Nd AND Rb–Sr WHOLE-ROCK ISOTOPIC DATA, LIVRADOIS SUITE, FRENCH MASSIF CENTRAL

Lithology	Sample number	$^{143}\text{Nd}/^{144}\text{Nd}$ corr.	error $^{143}\text{Nd}/^{144}\text{Nd}$	$\xi\text{Nd}$ spectro	[Nd] ppm spectro	$^{144}\text{Nd}$ nm/g	Sm ppm spectro	$^{147}\text{Sm}$ nm/g	$^{147}\text{Sm}/^{144}\text{Nd}$	$^{143}\text{Nd}/^{144}\text{Nd}$ at 300 My	$\xi\text{Nd}$
Two-mica leucogranite	8	0.512054	0.000009	-12.30	18.89	31.17	3.299	3.31	0.106	0.511846	-7.42
Two-mica leucogranite	152	0.512088	0.000011	-11.64	15.49	25.55	3.243	3.25	0.127	0.511838	-7.57
Two-mica leucogranite	SGL2K14	0.512072	0.000014	-11.95	18.49	30.50	3.254	3.26	0.107	0.511862	-7.10
Two-mica leucogranite	SLG2K12	0.511979	0.000043	-13.77	9.99	16.48	1.927	1.93	0.117	0.511749	-9.31
Paragneiss	SGL2K24	0.512046	0.000014	-12.46	34.27	56.53	6.113	6.13	0.108	0.511833	-7.67
Paragneiss	SGE01157	0.512003	0.000017	-13.31	35.78	59.02	6.154	6.17	0.104	0.511798	-8.36
Diatexite	F82a	0.512078	0.000019	-11.84	24.39	40.23	4.790	4.80	0.119	0.511844	-7.46
Diatexite	F84	0.512049	0.000016	-12.41	30.33	50.03	5.766	5.78	0.115	0.511822	-7.88
Porphyritic monzogranite	155e	0.512053	0.000011	-12.33	46.28	76.35	6.684	6.70	0.088	0.511881	-6.74
Porphyritic monzogranite	155b	0.512134	0.000017	-10.76	43.89	72.40	7.975	7.99	0.110	0.511917	-6.03
MME	SGW79c	0.512194	0.000018	-9.58	65.41	107.89	14.332	14.36	0.133	0.511933	-5.73
MME	155c	0.512062	0.000013	-12.14	58.45	96.42	9.515	9.53	0.099	0.511868	-6.99

Lithology	Sample number	$^{87}\text{Sr}/^{86}\text{Sr}$	error in $^{87}\text{Sr}/^{86}\text{Sr}$	[Sr] ppm	$^{86}\text{Sr}$ nm/g	Rb ID ICPMS-ID	$^{87}\text{Rb}$ moles	$^{87}\text{Rb}/^{86}\text{Sr}$	$^{87}\text{Rb}/^{86}\text{Sr}$ initial*
Two-mica leucogranite	8	0.743700	0.000027	106.28	119.21	218.59	7.12E-07	5.9747	0.718193
Two-mica leucogranite	152	0.736211	0.000026	134.37	150.84	210.68	6.86E-07	4.5512	0.716782
Two-mica leucogranite	SGL2k12	0.733962	0.000018	120.37	135.14	171.05	5.57E-07	4.1242	0.716355
Paragneiss	SGL2K24	0.724662	0.000014	179.81	202.07	160.55	5.23E-07	2.5889	0.713610
Paragneiss	SGE 01 157	0.722314 0.000074	0.000028	169.10	190.08	93.51	3.05E-07	1.6030	0.715471
Diatexite	F84	0.727419	0.000027	186.51	209.55	182.39	5.94E-07	2.8361	0.715312
Porphyritic monzogranite	155e	0.719059	0.000028	360.98	405.89	198.81	6.48E-07	1.5960	0.712245
Porphyritic monzogranite	155b run 3	0.718459	0.000017	426.17	479.22	230.14	7.50E-07	1.5648	0.711779
MME	sgw79c run3	0.719375	0.00002	350.64	394.25	198.89	6.48E-07	1.6438	0.712357
MME	155c run2	0.721687	0.000040	323.50	363.65	248.16	8.09E-07	2.2236	0.712194

\* Initial  $^{87}\text{Rb}/^{86}\text{Sr}$  value at 300 million years. MME: microgranular mafic enclave.

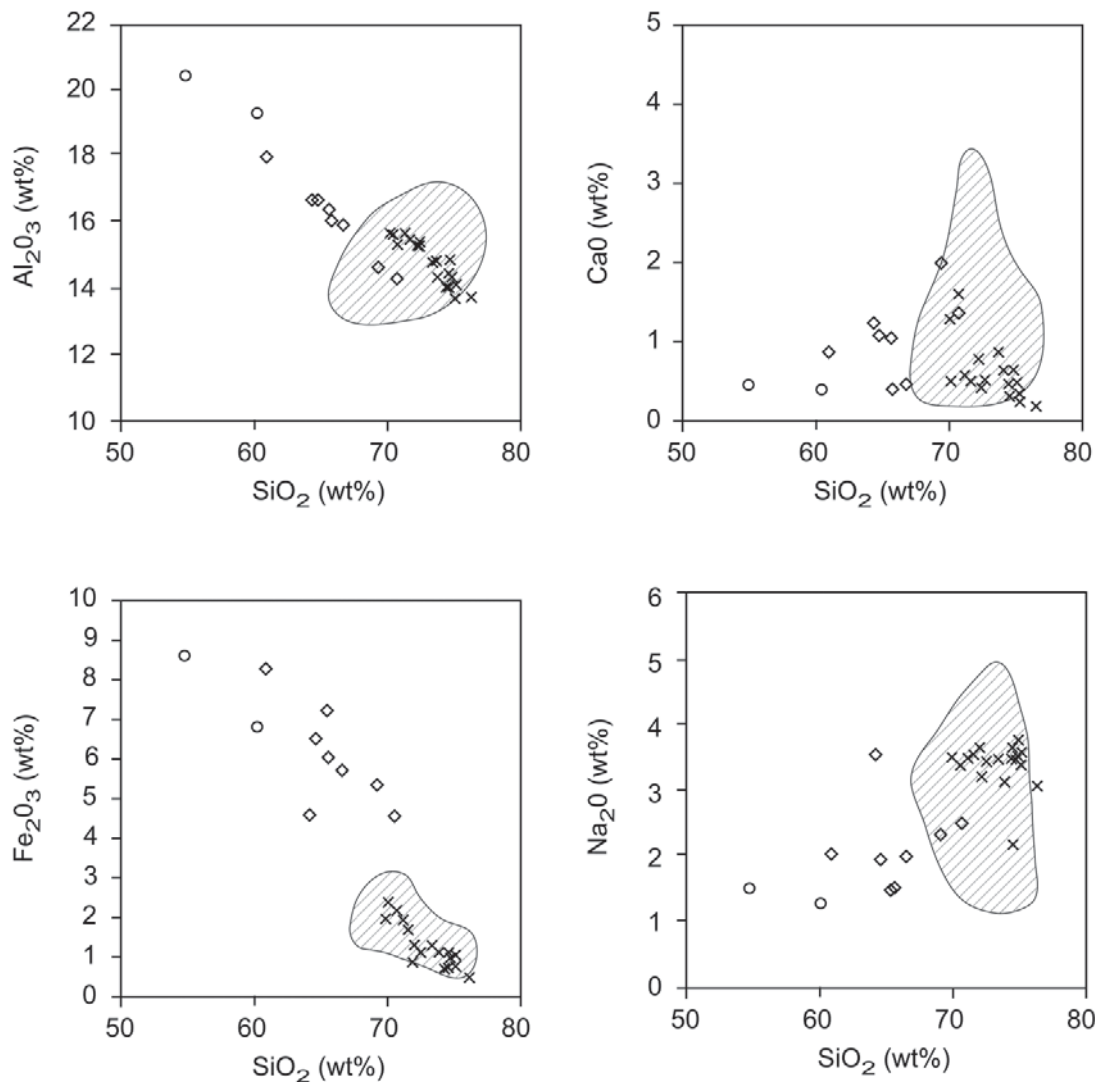


FIG. 7. Selected Harker variation diagrams in which we compare the composition of anatectic metasedimentary rocks: meta-texite paragneiss and diatexite migmatite ( $\diamond$ ), enclaves of paragneiss ( $\circ$ ) and two-mica leucogranites ( $\times$ ). The hatched zone corresponds to a compilation of melt compositions obtained from the partial fusion of pelite (Gardien *et al.* 1995, Patiño Douce & Harris 1998, Patiño Douce & Johnston 1991). The correlation for all the values of the samples is consistent with the possible partial fusion of the anatectic metasedimentary rocks.

#### *Interpretation of porphyritic monzogranite and associated MME*

The porphyritic monzogranite is weakly peraluminous, with A/CNK values in the range 1.06–1.07, but is rich in Mg (~2 wt% MgO), Fe (~4 wt% Fe<sub>2</sub>O<sub>3</sub>) and K (~4.5 wt% K<sub>2</sub>O). Thus, the porphyritic monzogranite falls within the group of plutonic rocks described as having high K–Mg by Laporte *et al.* (1991). The MME,

although more mafic than the porphyritic monzogranite, also display a similar high K–Mg signature (A/CNK 1.01 to 1.04, ~3.5 wt% MgO, ~7 wt% Fe<sub>2</sub>O<sub>3</sub>, ~3 wt% K<sub>2</sub>O). The origin of high K–Mg magmas is not well understood; some authors contend that these magmas are mixtures of mantle- and crust-derived magmas (Barbarin 1999, Laporte *et al.* 1991). Although the high contents of compatible elements do point to a mantle-derived component, the high K<sub>2</sub>O and LILE contents

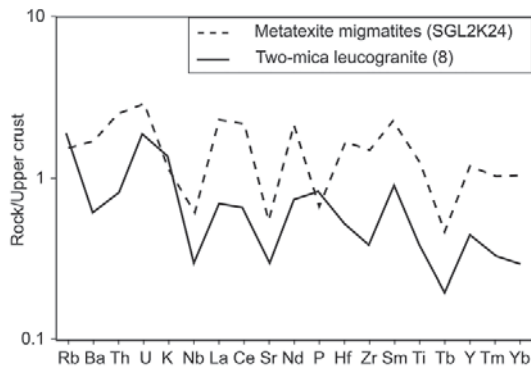


Fig. 8. Upper-crust-normalized multi-element patterns; values for the upper crust are taken from Taylor & McLennan (1981). Representative sample for anatectic rocks (dashed line) and two-mica leucogranite are compared. For the majority of trace elements, concentrations are higher in the anatectic rocks. The concentration of “incompatible” elements in the anatectic rocks is consistent with the mineralogy and the presence of accessory minerals such as zircon, or monazite.

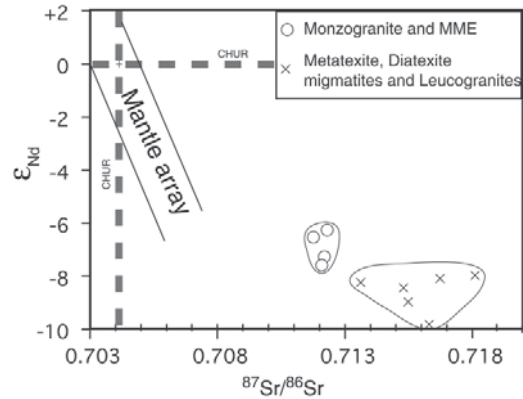


Fig. 9. Plot of  $\epsilon_{Nd}$  versus  $^{87}Sr/^{86}Sr$ , with values recalculated to 300 Ma. The porphyritic monzogranite and MME have some values intermediate between those observed for the migmatitic paragneiss and the two-mica leucogranite, and those for the mantle array.

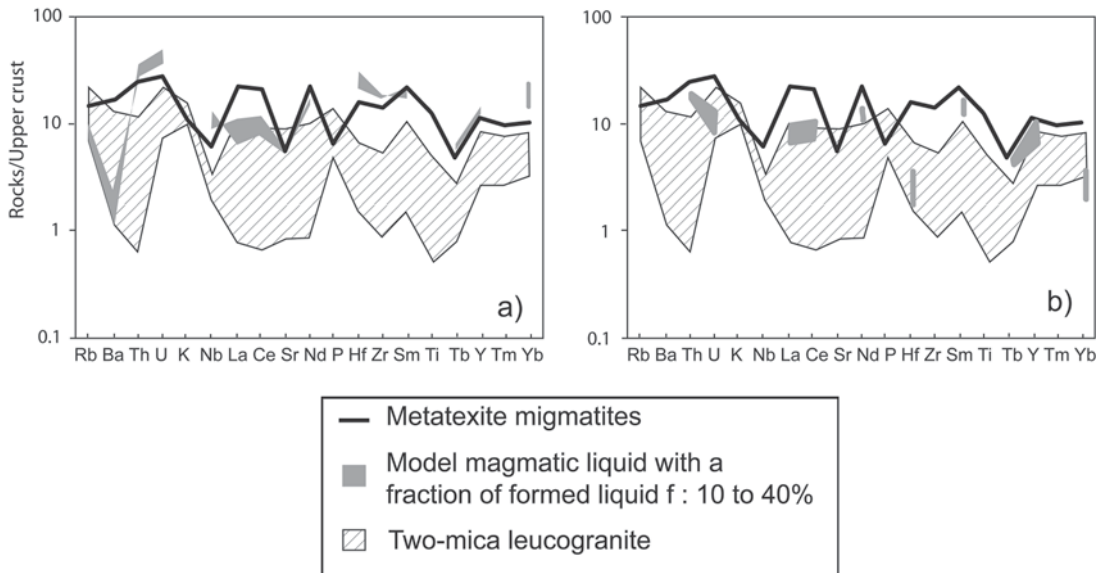


Fig. 10. Result of the modeling of partial melting of paragneiss. (a) Restite: 65% biotite, 15% plagioclase, 10% quartz, 5% K-feldspar. (b) Restite: 64% biotite, 15% plagioclase, 10% quartz, 5% K-feldspar, 1% zircon. The model including zircon in the restite is more consistent with the pattern observed for the two-mica leucogranite. The field of stability of all the accessory minerals of the anatectic rocks is important during the partial melting.

suggest either a very peculiar (*i.e.*, strongly enriched) mantle, or the presence of a crustal component. Figures 11a and 11b show that the data for the porphyritic monzogranite lie between the two-mica leucogranite

and the MME. Because the petrographic features of the porphyritic monzogranite support a hybrid origin, mixing lines between the MME and two-mica leucogranite, shown on Figure 11, indicate the proportion of

mafic magma required to mix with a leucocratic two-mica magma to produce the porphyritic monzogranite. The compositions for the two MME samples differ; we have chosen the sample that we believe more closely represents the primitive (least-contaminated) mafic magma for the mixing line.

The porphyritic monzogranite and its MME are both rich in compatible elements (*e.g.*, Ni ~30 and ~100 ppm; Cr ~100 and ~500 ppm, respectively) and in incompatible elements (LILE) (*e.g.*, Rb ~200 ppm for monzogranite and MME: Table 1). Typically, they also have rather high HFSE contents (*e.g.*, between 13 and 25 ppm Nb, and ~20 ppm Y). Figure 11c shows in a binary diagram amounts of Nb *versus* Rb. As for major

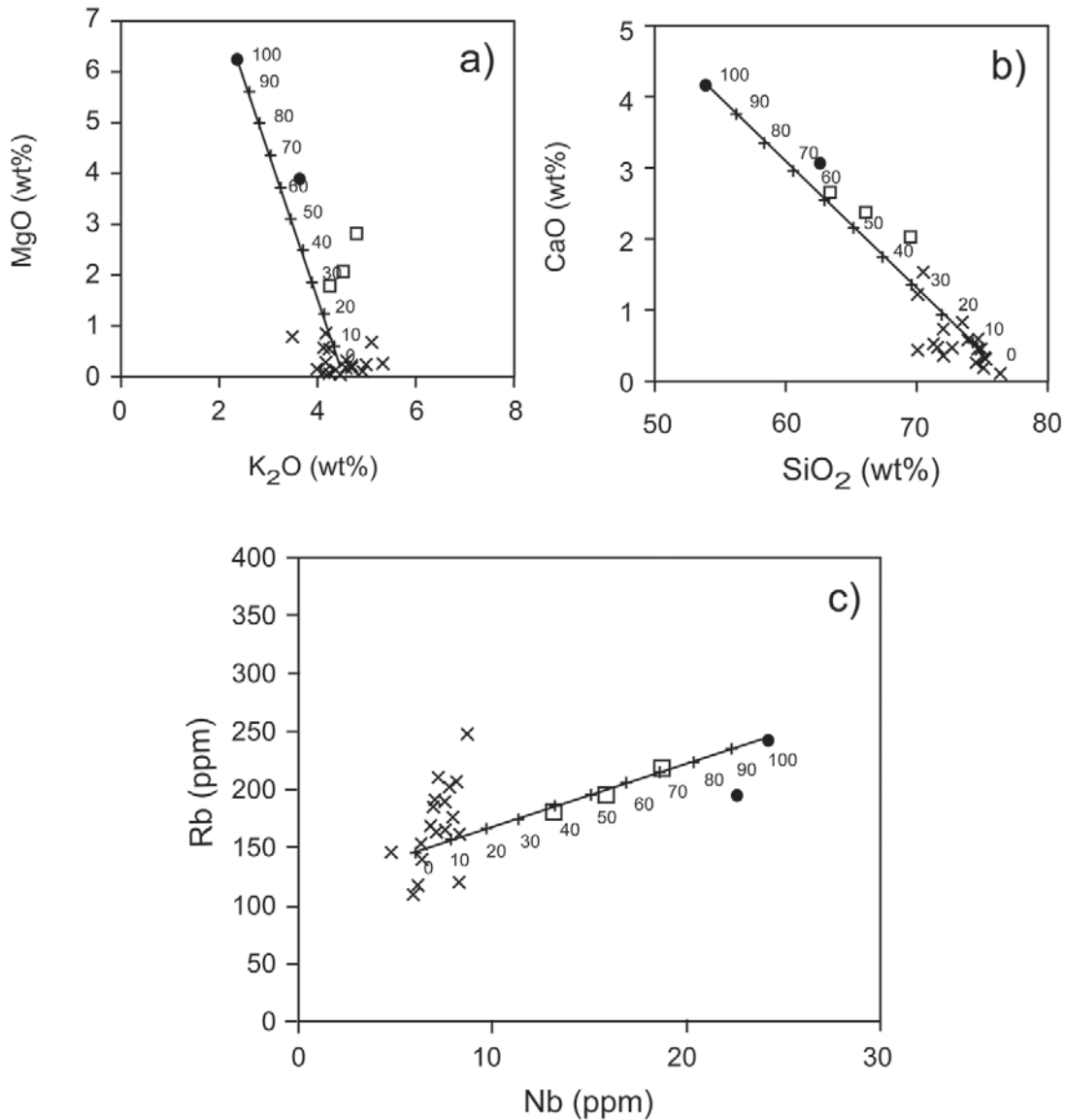


FIG. 11. Selected major- and trace-element diagrams showing the composition of the porphyritic monzogranites ( $\square$ ) in relation to the composition of the MME ( $\bullet$ ) and the leucogranites ( $\times$ ). a) K<sub>2</sub>O *versus* MgO, b) SiO<sub>2</sub> *versus* CaO, and c) Rb *versus* Nb. The (+) symbols represent a mixing curve at 10% intervals with mafic magma represented by the geochemistry of the enclave.

elements, the data for the porphyritic monzogranite, the two-mica leucogranite, and the MME are colinear. All other binary diagrams for trace elements gives the same colinear relationship, which strongly suggests a mixing process.

The REE patterns for the porphyritic monzogranite and its MME have similar shapes, but the MME have the higher abundances. Both are LREE-enriched (~50 ppm La), display a moderate negative Eu anomaly, and are moderately fractionated ( $La/Yb_N \approx 20$ ).

#### *Rb/Sr and Sm/Nd isotopic data*

The porphyritic monzogranite and the MME have similar age-corrected (300 Ma) Sr and Nd isotopic ratios. This similarity arises because MME is not representative of the initial mafic magma; it could have re-equilibrated with the porphyritic monzogranite. The isotopic compositions of these rocks lie between those of the migmatites, the two-mica leucogranites, and the mantle array (Fig. 9). This observation precludes derivation solely from a local crustal source and strongly implicates the mantle in their creation.

#### GEOCHEMICAL MODELING OF THE PETROGENESIS OF THE PORPHYRITIC MONZOGRANITE

The geochemical evidence suggests that the porphyritic monzogranite represents a hybrid magma; a component derived from a potentially enriched mantle source mixed with anatectic melt derived from local metasedimentary rocks. This conclusion is consistent with both the field (porphyritic intrusive body in a partially molten crust) and petrological evidence (grain size, zoning in plagioclase). The mixed magma model will now be tested using geochemical modeling.

The most likely (available) felsic end-member for the mixing in the model is a magma similar to the two-mica leucogranite of the area. Although the MME may already represent hybrid magmas between a "true" mafic magma and the host granite, we use the composition of the MME to model the mafic magma end-member.

Magma mixing can be modeled by the simple mass-balance equation:

$$C_m = \gamma C_a + (1 - \gamma) C_b \quad (1)$$

where  $C_m$  is the concentration of an element in the mixture (taken to be the porphyritic monzogranite),  $C_a$  is the concentration of an element in one end-member of the mixture (the MME),  $C_b$  is the concentration of an element in the other end-member (the two-mica leucogranite), and  $\gamma$  is the mass fraction of the mafic end-member in the mixture.

Following the "mixing test" of Fourcade & Allègre (1981), we rewrite this equation as

$$C_m - C_b = \gamma (C_a - C_b) \quad (2)$$

In a  $(C_a - C_b)$  versus  $(C_m - C_b)$  diagram, if the rock "m" is indeed a mixture of end members "a" and "b", then representative points for all the major elements should plot along a straight line passing through the origin, the slope of which corresponds to  $\gamma$ .

In our case, a mixture of 70% MME and 30% leucogranite (Fig. 12a) fits the measured major-element compositions. This mixture is also tested for the REE (Fig. 12b), and yields a modeled REE pattern very close to that of the porphyritic monzogranite (Table 1). Small differences in Eu could be related to the separation of feldspar and melt, evidence for which can be seen in outcrop. The accumulation of feldspar is also suggested by the misfit for  $Al_2O_3$  on the mixing diagram (Fig. 12a).

#### DISCUSSION

Two coexisting magmas were present in the Livradois region at ca. 300 Ma: (1) the two-mica leucogranite suite genetically linked to the nearby migmatites, and (2) the porphyritic monzogranite, a high K-Mg magma formed by mixing between a mafic component represented by the MME, and an anatectic melt similar to the two-mica leucogranite.

#### *Crustal anatexis and formation of the leucogranitic melts*

The peraluminous composition of the two-mica leucogranite suggests that it was derived from a pelitic protolith, a conclusion consistent with most of the experimental work on leucogranites (Patiño Douce & Johnston 1991, Vielzeuf & Holloway 1988). The modeling shows that the paragneiss in the study area is a permissible source for the leucogranite. The fact that accessory minerals are only a minor component of the leucogranite indicates that most of the accessory phases remained in the residue. There are two possible reasons for this. (1) The temperature during partial melting was relatively low; as a result, the accessory minerals did not dissolve into the partial melt. For example Montel (1993) showed that the solubility of monazite in the melt is an exponential function of temperature. Moreover, at low temperatures and a low degree of melting, the solid fraction predominates and acts as a filter to trap the accessory phases. (2) The accessory minerals were included in the major minerals and, therefore, inaccessible to melt (Watson *et al.* 1989). Indeed, the biotite in the migmatites contains a very high proportion of accessory minerals, which would have isolated them from the anatectic melt.

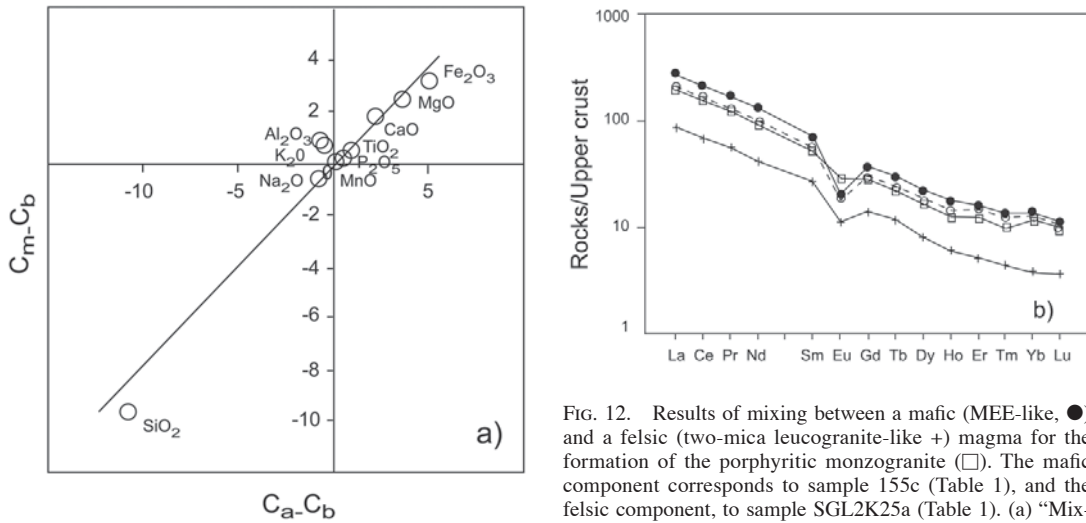


FIG. 12. Results of mixing between a mafic (MEE-like, ●) and a felsic (two-mica leucogranite-like +) magma for the formation of the porphyritic monzogranite (□). The mafic component corresponds to sample 155c (Table 1), and the felsic component, to sample SGL2K25a (Table 1). (a) "Mixing test" of Fourcade & Allègre (1981) for major elements, showing that the major-element composition of the porphyritic

monzogranite is consistent with the mixing of 70% of mafic end-member and 30% of the felsic end-member. The  $R^2$  coefficient in this case is 0.95. (b) The REE profile of a mixture of 70% of the mafic component 155c and 30% of a felsic component SGL2K25. The dashed line (○) corresponds to the model, and is compared to the real composition of the porphyritic monzogranite (□) 155b (Table 1).

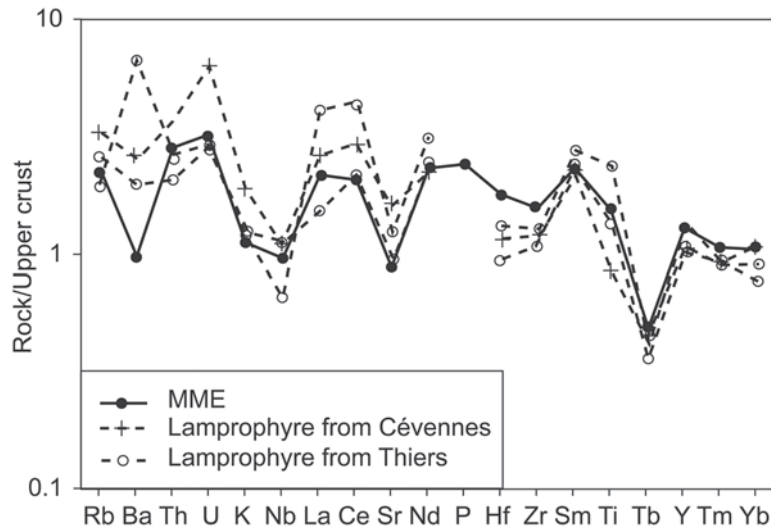


FIG. 13. Spider diagrams normalized to upper crust (Taylor & McLennan 1981) for MME (●) compared to lamprophyres from Cévennes (+) and Thiers (○) (Agranier 2001). The patterns for all rocks are similar, and suggest the same origin for the mafic magma that forms these rocks.

*Origin of the mafic components  
in the porphyritic monzogranite*

The source of the MME and the mafic component in the porphyritic monzogranite could be either the mantle, or the lower crust. The nature of the Hercynian lower crust is known from xenoliths in nearby Cenozoic volcanos, such as the Bournac pipe, 80 km southeast of our study area (Dostal *et al.* 1980, Downes *et al.* 1990). The xenolith suite includes mafic granulites (47 < SiO<sub>2</sub> < 54 wt%), felsic granulites, and metasedimen-

tary rocks. Furthermore, Dostal *et al.* (1980) found that the Hercynian lower crust is significantly depleted in incompatible elements, LILE, REE, and HFSE. Thus, the low-SiO<sub>2</sub> mafic and enriched incompatible element nature of the MME is not consistent with derivation from the known Variscan lower crust in the Massif Central. A spidergram (Fig. 13) for the incompatible elements shows the chemical similarity between the MME and Hercynian lamprophyre dykes that are of about the same age, from the Thiers area 50 km to the north, and from the Cévennes area, 120 km to the south

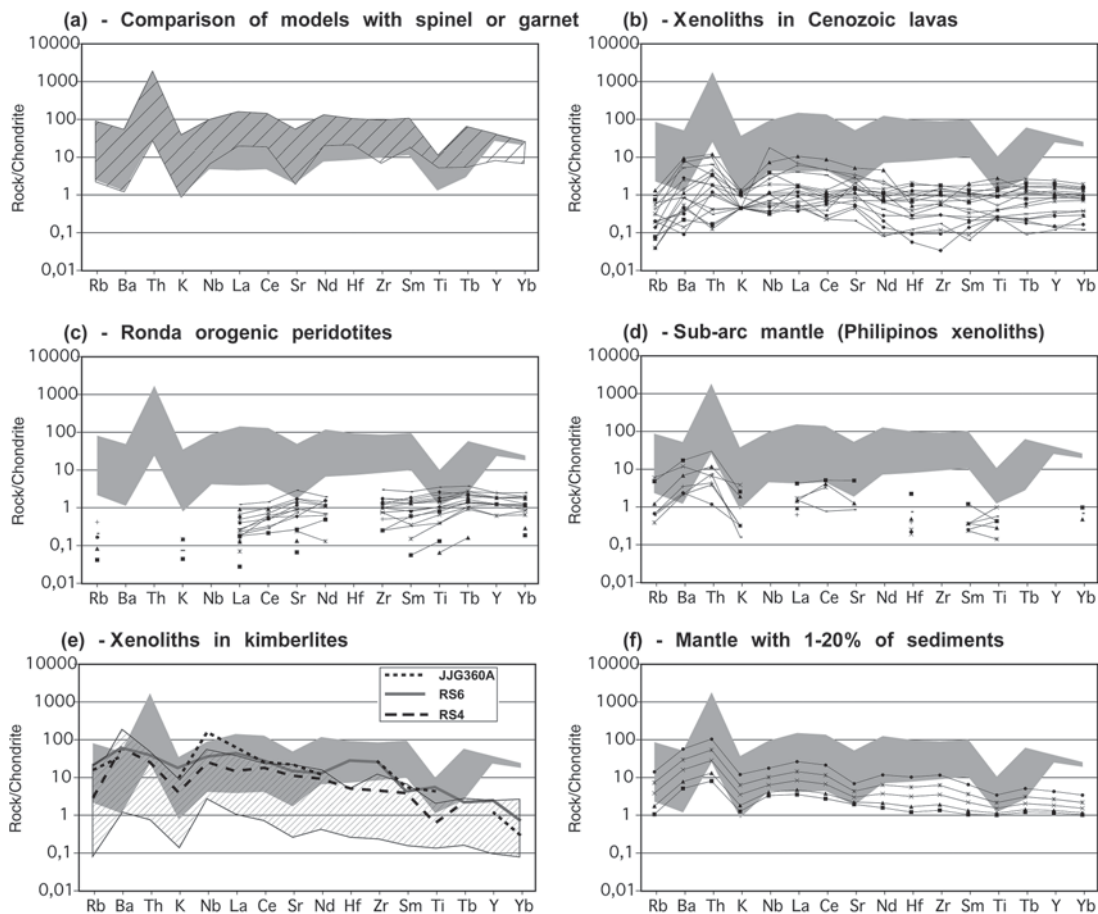


FIG. 14. Chondrite-normalized (Sun *et al.* 1989) multi-element diagrams for possible compositions of the mantle source. In all diagrams, the shaded area is the field of recalculated mantle compositions (see text for details) and is compared with various peridotite samples. (a) Comparison between the recalculated compositions of mantle and a mantle with residual garnet (shaded) or spinel (hachured). (b) Massif Central xenoliths in recent (Tertiary and Quaternary) lavas (Lenoir *et al.* 2000). (c) Orogenic peridotites, Ronda (Frey *et al.* 1985). (d) Sub-arc mantle, xenoliths in recent Philippine lavas (Maury *et al.* 1992). (e) Peridotitic xenoliths in kimberlites (hachured field from Erlank *et al.* 1987, Menzies *et al.* 1987, Nixon *et al.* 1981, Rhodes & Dawson 1975, Rudnick *et al.* 1993, Winterburn *et al.* 1990). The thick lines correspond to three samples from Bultfontein pipe, samples RS4 and RS6 from Menzies *et al.* (1987) and sample JG360A from Erlank *et al.* (1987). (f) Mixing of Massif Central xenolithic mantle with 1–20% sediments (average Post-Archaean shale of Taylor & McLennan 1985).

in the Massif Central (Agranier 2001). Although the exact origin of lamprophyres is much debated, there is little doubt that they are mantle-derived melts. The degree of enrichment in trace elements shown by the MME and lamprophyres (100 to 1000 times chondritic, *i.e.*, 10–100 times MORB (Hart & Zindler 1986) implies a very enriched mantle source.

Modeling the melting of the mantle can be difficult, because of the large number of possible compositions for the source. Thus, we have used an inverse approach and calculated the composition of the mantle source that will yield a mafic partial melt with a composition similar to the MME. The results are given in Figure 14. This hypothetical mantle (1) is enriched between five and 30 times chondrite and, (2) initially has prominent positive anomalies in Th (and U), and negative anomalies in K, Sr and Ti. Which Al-rich phase is present in such a mantle, whether garnet or spinel, is not important (Fig. 14a) for the distribution of the HFSE and HREE, except to a limited extent. This model uses equilibrium batch-melting, but the choice of melting mode is not particularly critical. Modeling with other modes of melting does affect the resulting compositions, but the differences between them are minor (Maaløe 1985) except, perhaps, at low fractions of melt. In all instances, these differences are small enough not to affect the interpretations below.

The composition of the model source can be compared with real mantle (Figs. 14b to f). Peridotites are known from the Massif Central as enclaves in Cenozoic basalts (Lenoir *et al.* 2000) and show a depletion in most incompatible elements (Fig. 14b), as indicated by a concave trace-element pattern. They are also an order of magnitude too depleted in most trace elements to be a viable source for the MME. Seismic tomography shows that Cenozoic volcanism in the Massif Central is linked to the rise of the asthenospheric (or even lower) mantle (*e.g.*, Goes *et al.* 1999, Granet *et al.* 1995). Therefore, the Cenozoic peridotites do not represent the subcontinental mantle that existed under the Massif Central in late Hercynian times. Orogenic peridotites from the Ronda massif (Frey *et al.* 1985) are even more depleted than the Massif Central peridotites (Fig. 14c), and cannot be representative of the mantle source either.

Maury *et al.* (1992) have described nodules of metasomatized peridotite that occurs as enclaves in calc-alkaline lavas from the Philippines. They consider these to represent sub-arc metasomatized mantle. Mantle from such a tectonic setting could make a realistic source of enriched mantle in a collision setting. However, as Figure 14d shows, these rocks cannot be construed to be a realistic source either, as they reach only the lower envelope of suitable compositions of mantle.

The only peridotites from the literature that have an adequate degree of enrichment are the enclaves of old subcontinental lithosphere found in kimberlite (Fig. 14e). Although, old, enriched, subcratonic mantle

is a possible source, evidence in Western Europe for a pre-existing craton, with its associated enriched mantle, is currently lacking. There are two possibilities: (1) the old subcratonic mantle was not present, or (2) this enriched mantle signature is lost when the lithosphere beneath the Variscan orogen became delaminated.

We suggest a composite source with both mantle and enriched crustal components (Fig. 14f). This mixture of the old subcratonic mantle could occur before the Variscan orogeny. The composition such a composite source was estimated by adding between 1 and 20% sediments to the mantle. Such a source has been proposed for compositionally similar magmas, such as the K–Mg-rich lamprophyre, the so-called vaugnerites, that are widespread in the Massif Central (Michon 1987, Montel & Weisbrod 1986). The initial trace-element composition of the mantle is largely irrelevant in this model, because the crustal component is enriched in incompatible elements by one or two orders of magnitudes over the mantle. We have used the post-Archean shale of Taylor & McLennan (1985) as the crustal component. The mixture shows a degree of enrichment comparable with the proposed source (Fig. 14f). Furthermore, the shape of the trace-element patterns is also consistent with the anticipated positive Th, and negative K, Sr and Nd anomalies, and plateaus for Nb to Ce and Nd to Sm. The geological circumstances in which such mixing may occur are discussed below.

#### *Constraints from Rb/Sr and Sm/Nd isotopic and trace-element data*

The highly enriched signature shown by the porphyritic monzogranite and its MME can be interpreted in one of four ways.

(1) The isotopic signature is entirely due to mixing between a leucogranitic magma (representation of a two-mica granite) related to *in situ* melting and a mantle-derived mafic magma. Curve (b) in Figure 15 shows that mixing of the two-mica leucogranite and a mafic magma with a CHUR-like isotopic composition can account for the signature of the porphyritic monzogranite and its MME. Between 50 and 60% leucogranitic magma is required, in good agreement with the mixing model presented earlier. In this scenario, the MME would have had to undergo complete isotopic re-equilibration with their host. However, we regard this process as rather unlikely. First, rocks more primitive than the MEE do not occur in the study area. Second, the lamprophyres in the region probably are devoid of any influence from the upper crust, yet have enriched isotopic characteristics, albeit to a lesser degree (Agranier 2001, Turpin *et al.* 1988). The leucogranitic melts are considered to have been relatively depleted in most incompatible trace elements; for example, they contained 20 ppm of La, whereas the MME have 65 ppm. Consequently, if the MME are the product of mixing between a mafic magma and the leucogranitic

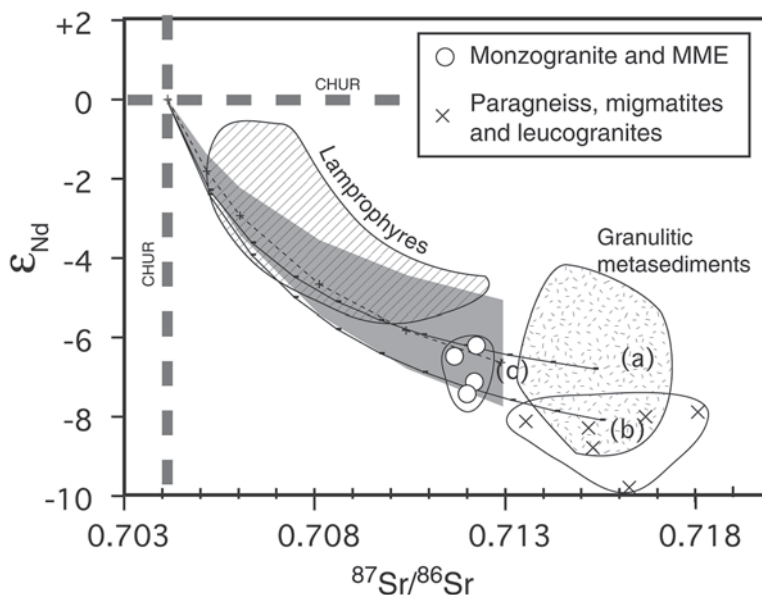


FIG. 15. Plot of  $\epsilon_{\text{Nd}}$  versus  $^{87}\text{Sr}/^{86}\text{Sr}$ , with all values recalculated at 300 Ma unless specified otherwise. Hachured field of lamprophyres (all Massif Central) after Turpin *et al.* (1988) and Agranier (2001), recalculated at the time of emplacement, different for each sample but between 310 and 320 Ma. Stippled field of granulite metasediments (Bournac, 50 km southeast of study area) after Downes *et al.* (1990). (a) Assimilation of granulitic lower crust by a mafic magma with CHUR-like isotopic characteristics (ticks correspond to 10% increments). (b) Mixing between Livradois metasediments and a mafic magma with CHUR-like isotopic characteristics (ticks correspond to 10% increments). (c) Shaded field is the isotopic composition (recalculated at 315 Ma) of a CHUR-like mantle into which sediments have been mixed at 420 Ma. Isotopic composition of the sediments are taken from the pre-Devonian sediments from the Montagne Noire area, 250 km to the south of the study area (Simien *et al.* 1999). Dashed line correspond to the values at 315 Ma for a mixture with sediments with  $\epsilon_{\text{Nd}}(420 \text{ Ma}) = -6$ ; ticks correspond to the proportion (1, 2, 5, 10 and 20%) of sediments mixed with a CHUR-like mantle. Limits of the shaded field correspond to models calculated at 315 Ma, using sediments with  $\epsilon_{\text{Nd}}(420 \text{ Ma})$  between  $-4$  to  $-8$ .

melt, this mafic magma should be even more enriched. Therefore, we think that the enriched character of the MME is related to the source, and not to interactions with anatectic melt in the middle crust.

(2) The isotopic signature is composite, and related to the interactions between a CHUR-like or depleted mantle and the granulite-facies lower crust during ascent of the magma. Figure 16 shows that granulite-facies lower crust in the Massif Central has interelement values (*e.g.*, La/Yb and Ba/Sr) that preclude it as a source component. Assimilation of lower crust in general will not result in an enriched mafic magma. The very radiogenic signature of the lower crust, however (Downes *et al.* 1990), could account for an isotopically enriched magma. Quantitative modeling (Fig. 15, curve a) indicates that assimilation of the lower crust can indeed yield the correct isotopic signature, but it

requires such large amounts of lower crust material (60 to 80%) to be added that the whole-rock composition becomes unrealistic. Therefore, interactions between mafic magma and the Variscan lower crust cannot be the principal cause of enrichment of the mafic magmas.

(3) The mantle source had an enriched signature. This hypothesis is consistent with conclusions drawn from trace-element profiles in the MME and implies the existence of an old subcontinental lithospheric mantle beneath the continents involved in the Hercynian collision. The problem is that old (Proterozoic) lithospheric components are not known from the Hercynian belt (Liew & Hofmann 1988), although omnipresent mid-Proterozoic Nd model ages (Downes & Duthou 1988, Downes *et al.* 1997, Simien *et al.* 1999) suggest that it might well have existed.

(4) The mantle source itself could contain a mixture of components. The isotopic composition (at 300 Ma) of a CHUR-like mantle to which 1 to 20% of sediments were mixed at 420 Ma, the time at which subduction occurred under the Massif Central, has been plotted on Figure 15 (curve and field c). Such a process is able to produce a radiogenic source with isotopic signatures consistent with the present-day signature of the MME.

The isotopic evidence alone is equivocal (Agranier 2001, Pin *et al.* 1990, Turpin *et al.* 1988). However, the combination of trace-element and isotopic information suggests that the most likely origin for the MME and porphyritic monzogranite is an enriched source, made of a mantle mixed with crustal material.

What causes enrichment of the mantle is poorly known; different mechanisms have been proposed for different geological settings and for different types of K- and Mg-enriched magmas. The crustal component has been ascribed to slab-released fluids (Wyllie 1987),

percolation of mafic magmas (Bodinier *et al.* 1990, Van derWal & Bodinier 1996), or metasomatism by felsic melts (Martin *et al.* 2005, Moyen *et al.* 2001). We have already argued that sediments were added to the mantle to produce an enriched source; next we discuss how that might have occurred.

The subduction of sediments and their recycling back into the deep mantle are now well documented (*e.g.*, Plank & Langmuir 1998). Subduction under the Massif Central occurred at about 400 Ma (Paquette *et al.* 1995, Pin & Lancelot 1982). At this time, pelagic sediment, or sediment from the accretionary prism could have been subducted into the mantle, and an enriched mantle wedge formed near, or above, the descending plate. The sediments possibly were mechanically interleaved with the mantle rocks. Similar models for enrichment of the mantle have been proposed by investigators of ultrapotassic, synconvergent magmatism elsewhere (Bachinski & Scott 1979, Venturelli *et al.* 1984).

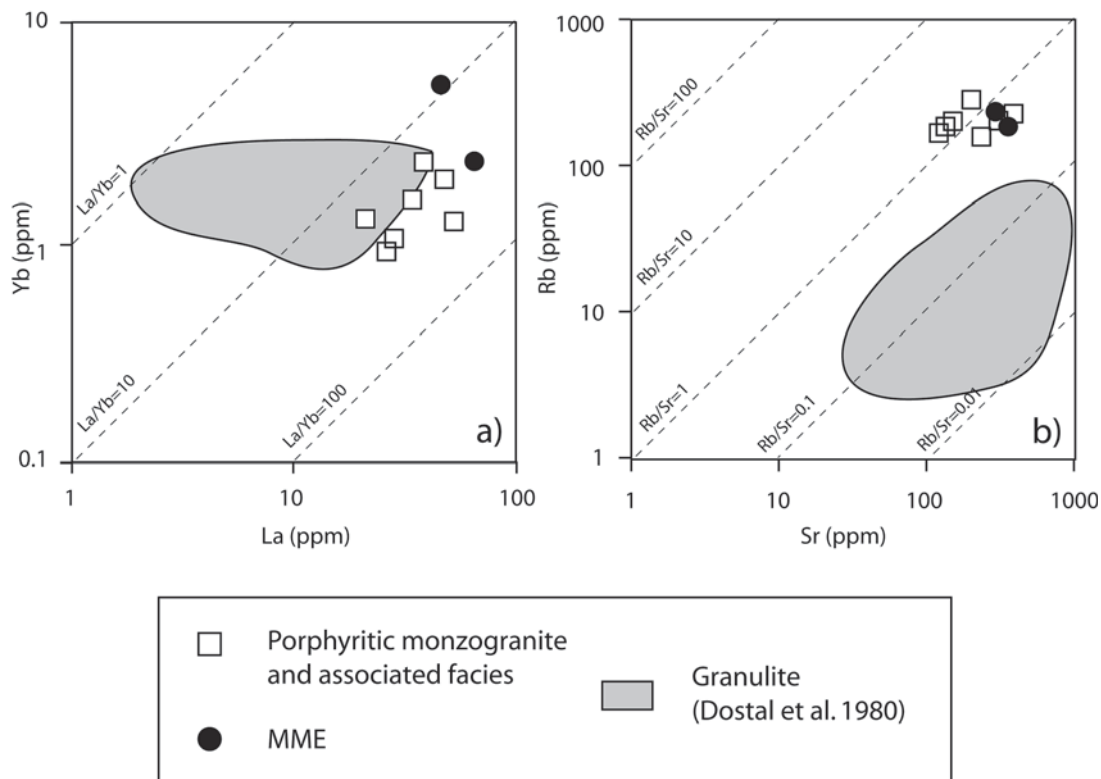


FIG. 16. Influence of the lower crust granulites (Dostal *et al.* 1980; grey domains) in the source of the mafic component of the porphyritic monzogranite (open squares). In a La versus Yb diagram (a), the Mg–K series is more enriched than the granulite, with higher La/Yb values. Interactions of a mantle-derived melt with lower crust granulites is, therefore, unable to generate the observed composition of melt. In the Sr versus Rb diagram (b), granulites show Rb/Sr values that are too low to be the source of enrichment, and that addition of mantle peridotite (see text and Fig. 14) is unable to generate the expected signature. Black circles: mafic microgranular enclaves.

The crustal material added to the mantle need not be restricted to subducted sediments. The subduction of felsic continental fragments has also been documented in the Alpine belt (Chopin *et al.* 1991, Reinecke 1991), and has been suggested for the Hercynian belt (Lardeaux *et al.* 2001). Indeed, if continental crust is subducted to sufficient depth that it undergoes partial melting, then such anatectic magmas could ascend into overlying mantle-wedge (Rapp *et al.* 1999) and make an enriched mantle.

#### *Cause of partial melting in the Massif Central*

The generation of migmatites, two-mica granites, porphyritic monzogranite (K–Mg granite) and the mafic magmas from which the MME were derived occurred in the short span between 350 and 290 Ma. Thus, the partial melting that affected the crust and the mantle coincided with the transition from contractional to extensional deformation in the orogen. Nelson (1992) suggested that the change from contraction to extension in orogens is triggered by the detachment and foundering of the subducted oceanic lithosphere, and possibly the lithosphere under the upper plate, following their transformation to dense eclogite. The removal of the dense root enables the rapid uplift of the less dense, thickened continental crust, and relaxes the contractional forces. Detachment of the dense root allows new, hot mantle to rise under the orogen. The influx of hot mantle under the orogen heats the continental crust and triggers partial melting and the formation of granitic magma that characterizes the post-contraction stage of many orogens. The upwelling hot mantle may undergo decompression melting and generate mafic magmas that may intrude into the orogen and interact with the anatectic melts there.

Anatexis of the crust in the Massif Central produced metatexite migmatite and diatexite migmatite in the lower gneiss unit. Locally, domes of diatexite migmatite (*e.g.*, the Velay dome, just south of the study area) have risen through the upper gneissic unit. S-type granites formed by partial melting of pelitic metasediments occur throughout the Massif Central, generally as intrusive bodies (*e.g.*, Margeride and Guéret) in the migmatites, but also in the cores of dome structures, such as Velay. These bodies are the sites where the anatectic melts extracted from the lower gneiss unit have accumulated.

Mafic melts formed in the mantle at the same time and intruded into the partially molten crust, probably along active shear-zones (Brown & Solar 1998). The influx of mafic magma carried heat into the crust and locally increased the degree of partial melting; evidence comes from P–T paths of the orogen (Gardien *et al.* 1997), which show the late decompression and a high-temperature “excursion”. Therefore, these regions are loci of extensive interaction, mingling and mixing

between the mafic and crustal magmas (Castro *et al.* 2003), resulting in the formation of hybrid high-K–Mg magmas. Examples of high-K–Mg plutons in the Massif Central are the Bois Noirs and Saint-Julien-la-Vêtre plutons in the north, the Lozère massif, and the Aigoual-Saint-Guiral pluton in the south (Fig. 1). However, only in the Livradois area are they within the migmatites. Elsewhere, the plutons have risen sufficiently to intrude low-grade rocks. Therefore, the Livradois area provides a unique window to study how these magmas formed.

#### CONCLUSIONS

Two types of granite are present in the Livradois area, two-mica leucogranite, and a high-K–Mg porphyritic monzogranite. Petrological study and geochemical modeling suggest that the two-mica granites correspond to partial melts extracted from the nearby pelitic migmatites. In contrast, the porphyritic monzogranite formed by mixing between the two-mica granite and mantle-derived mafic melts. The mafic magmas were derived by partial melting of an enriched mantle that was probably created by the subduction and mechanical interleaving of metasedimentary rocks within the mantle some 50 to 70 Ma earlier.

The presence in the Livradois area of crustal melts that mixed with mafic magmas formed from an enriched mantle indicates that the phase of late-orogenic collapse coincided with a major episode of partial melting that affected the whole lithosphere under the Massif Central.

#### ACKNOWLEDGEMENTS

The authors are thankful to B. Bonin and an anonymous reviewer for their constructive suggestion and comments on the manuscript. We also thank D.B. Clarke for his helpful comments on an earlier version. This work was partially funded by the BRGM, as part of a project to produce 1:50 000 geological maps of France; the authors are grateful to P. Rossi for this support. Finally, we wish to thank C. Zimmermann and C. Parmentier of the isotope laboratory at CRPG Nancy for their help. This work represents part of an M.Sc thesis completed by F. Solgadi.

#### REFERENCES

- AGRANIER, A. (2001): *Un exemple de magmatisme ultrapotassique syn-orogénique: les lamprophyres du Massif Central Français. Approche géochimique et géochronologique*. Thèse D.E.A., Université Blaise Pascal, Clermont-Ferrand, France.
- ALLÈGRE, C.J. & MINSTER, J.F. (1978): Quantitative models of trace-element behavior in magmatic processes. *Earth Planet. Sci. Lett.* **38**, 1–25.

- BACHINSKI, S.W. & SCOTT, R.B. (1979): Rare-earth and other trace-element contents and origin of minettes (mica-lamprophyres). *Geochim. Cosmochim. Acta* **43**, 93-100.
- BARBARIN, B. (1988): Field evidence for successive mixing and mingling between the Piolard diorite and the Saint-Julien-La-Vetres monzogranite (Nord-Forez, Massif Central, France). *Can. J. Earth Sci.* **25**, 49-59.
- BARBARIN, B. (1999): A review of the relationships between granitoid types, their origins and their geodynamic environments. *Lithos* **46**, 605-626.
- BEA, F., MONTERO, P. & ORTEGA, M. (2006): A LA-ICP-MS evaluation of Zr reservoirs in common crustal rocks: implications for Zr and Hf geochemistry and zircon-forming processes. *Can. Mineral.* **44**, 693-714.
- BEA, F., PEREIRA, M.D. & STROH, A. (1994): Mineral/leucosome trace-element partitioning in a peraluminous migmatite (a laser ablation-ICP-MS study). *Chem. Geol.* **117**, 291-312.
- BODINIER, J.-L., VASSEUR, G., VERNIÈRES, J., DUPUY, C. & FABRIÈS, J. (1990): Mechanisms of mantle metasomatism: geochemical evidence from the Lherz orogenic peridotite. *J. Petrol.* **31**, 597-628.
- BONIN, B. (1990): From orogenic to anorogenic settings – evolution of granitoid suites after a major orogenesis. *Geol. J.* **25**, 261-270.
- BOUCHEZ, J.-L., DELAS, C., GLEIZES, G., NÉDÉLEC, A. & CUNEY, M. (1992): Submagmatic microfractures in granites. *Geology* **20**, 35-38.
- BROWN, M. (1973): The definition of metatexis, diatexis and migmatite. *Proc. Geol. Assoc.* **84**, 371-382.
- BROWN, M. & SOLAR, G.S. (1998): Shear-zone systems and melts: feedback relations and self-organization in orogenic belts. *J. Struct. Geol.* **20**, 211-227.
- BURG, J.-P., LEYRELOUP, A., MARCHAND, J. & MATTE, P. (1984): Inverted metamorphic zonation and large-scale thrusting in the Variscan Belt: an example in the French Massif Central. *Geol. Soc., Spec. Publ.* **14**, 47-61.
- CASTRO, A. (2001): Plagioclase morphologies in assimilation experiments: implications for disequilibrium melting in the generation of granodiorite rocks. *Mineral. Petrol.* **71**, 31-49.
- CASTRO, A., CORRETGÉ, L.G., DE LA ROSA, J.D., FERNÁNDEZ, C., LÓPEZ, S., GARCÍA-MORENO, O. & CHACÓN, H. (2003): The appinite-migmatite complex of Sanabria, NW Iberian massif, Spain. *J. Petrol.* **44**, 1309-1344.
- CHAPPELL, B.W. & WHITE, A.J.R. (1974): Two contrasting granite types. *Pac. Geol.* **8**, 173-174.
- CHOPIN, C., HENRY, C. & MICHARD, A. (1991): Geology and petrology of the coesite-bearing terrain, Dora-Maira Massif, Western Alps. *Eur. J. Mineral.* **3**, 263-291.
- CUNEY, M. & FRIEDRICH, M. (1987): Physicochemical and crystal-chemical controls on accessory mineral paragenesis in granitoids – implications for uranium metallogenesis. *Bull. Minéral.* **110**, 235-247.
- DIDIER, J. & BARBARIN, B. (1991): *Enclaves and Granite Petrology*. Elsevier, Amsterdam, The Netherlands.
- DINI, A., ROCCHI, S. & WESTERMAN, D.S. (2004): Reaction microtextures of REE–Y–Th–U accessory minerals in the Monte Capanne pluton (Elba Island, Italy): a possible indicator of hybridization processes. *Lithos* **78**, 101-118.
- DOSTAL, J., DUPUY, C. & LEYRELOUP, A. (1980): Geochemistry and petrology of meta-igneous granulitic xenoliths in Neogene volcanic rocks of the Massif Central, France – implications for the lower crust. *Earth Planet. Sci. Lett.* **50**, 31-40.
- DOWNES, H., DUPUY, C. & LEYRELOUP, A.F. (1990): Crustal evolution of the Hercynian belt of western Europe – evidence from lower-crustal granulitic xenoliths (French Massif-Central). *Chem. Geol.* **83**, 209-231.
- DOWNES, H. & DUTHOU, J.-L. (1988): Isotopic and trace-element arguments for the lower-crustal origin of Hercynian granitoids and pre-Hercynian orthogneisses, Massif Central (France). *Chem. Geol.* **68**, 291-308.
- DOWNES, H., SHAW, A., WILLIAMSON, B.J. & THIRLWALL, M.F. (1997): Erratum to “Sr, Nd and Pb isotopic evidence for the lower crustal origin of Hercynian granodiorites and monzogranites, Massif Central, France”. *Chem. Geol.* **140**, 289.
- DUPRAZ, J. & DIDIER, J. (1988): Le complexe anatectique du Velay (Massif Central français): structure d'ensemble et évolution géologique. *Géol. Fr.*, 73-88.
- DUTHOU, J.-L., CANTAGREL, J.M., DIDIER, J. & VIALETTE, Y. (1984): Paleozoic granitoids from the French Massif Central: age and origin studied by Rb<sup>87</sup> – Sr<sup>87</sup> system. *Phys. Earth Planet. Interior* **35**, 131-144.
- ERLANK, A.J., WATERS, F.G., HAWKESWORTH, C.J., HAGGERTY, S.E., ALLSOPP, H.L., RICKARD, R.S., MENZIES, M.A. (1987): Evidence for mantle metasomatism in peridotite nodules from the Kimberley pipes, South Africa. *In* Mantle Metasomatism (M.A. Menzies & C.J. Hawkesworth, eds.). Elsevier, London, U.K. (221-311).
- FOURCADE, S. & ALLÈGRE, C.J. (1981): Trace-elements behavior in granite genesis: a case-study the calc-alkaline plutonic association from the Querigut Complex (Pyrénées, France). *Contrib. Mineral. Petrol.* **76**, 177-195.
- FRANKE, W. (1989): Variscan plate-tectonics in Central-Europe – current ideas and open questions. *Tectonophysics* **169**, 221-228.
- FREY, F.A., SUEN, C.J. & STOCKMAN, H.W. (1985): The Ronda high-temperature peridotite: geochemistry and petrogenesis. *Geochim. Cosmochim. Acta* **49**, 2469-2491.

- GARDIEN, V., LARDEAUX, J.M., LEDRU, P., ALLEMAND, P. & GUILLOT, S. (1997): Metamorphism during late orogenic extension: insights from the French Variscan belt. *Bull. Soc. Géol. Fr.* **168**, 271-286.
- GARDIEN, V., THOMPSON, A.B., GRUJIC, D. & ULMER, P. (1995): Experimental melting of biotite + plagioclase + quartz  $\pm$  muscovite assemblages and implications for crustal melting. *J. Geophys. Res.* **B 100**, 15,581-15,591.
- GOES, S., SPAKMAN, W. & BIJWAARD, H. (1999): A lower mantle source for central European volcanism. *Science* **286**, 1928-1931.
- GRANET, M., WILSON, M. & ACHAUER, U. (1995): Imaging a mantle plume beneath the French Massif Central. *Earth Planet. Sci. Lett.* **136**, 281-296.
- HART, S.R. & ZINDLER, A. (1986): In search of a bulk-earth composition. *Chem. Geol.* **57**, 247-267.
- LAPORTE, D., ORSINI, J.B. & FERNANDEZ, A. (1991): Le complexe d'Ile-Rousse, Balagne, Corse du Nord-Ouest: pétrologie et cadre de mise en place des granitoïdes magnésio-potassiques. *Géol. Fr.* **4**, 15-30.
- LARDEAUX, J.M., LEDRU, P., DANIEL, I. & DUCHENE, S. (2001): The Variscan French Massif Central – a new addition to the ultrahigh pressure metamorphic “club”: exhumation processes and geodynamic consequences. *Tectonophysics* **332**, 143-167.
- LEDRU, P., LARDEAUX, J.M., SANTALLIER, D., AUTRAN, A., QUENARDEL, J.M., FLOCH, J.P., LEROUGE, G., MAILLET, N., MARCHAND, J. & PLOQUIN, A. (1989): Où sont les Nappes dans le Massif Central Français? *Bull. Soc. Géol. Fr.* **5**, 605-618.
- LENOIR, X., GARRIDO, C.J., BODINIER, J.-L. & DAUTRIA, J.M. (2000): Contrasting lithospheric mantle domains beneath the Massif Central (France) revealed by geochemistry of peridotite xenoliths. *Earth Planet. Sci. Lett.* **181**, 359-375.
- LIEW, T.C. & HOFMANN, A.W. (1988): Precambrian crustal components, plutonic associations, plate environment of the Hercynian fold belt of central Europe: indications from a Nd and Sr isotopic study. *Contrib. Mineral. Petrol.* **98**, 129-138.
- MAALØE, S. (1985): *Principles of Igneous Petrology*. Springer-Verlag, Berlin, Germany.
- MARTIN, H., SMITHIES, R.H., RAPP, R., MOYEN, J.-F. & CHAMPION, D. (2005): An overview of adakite, tonalite-trondhjemite-granodiorite (TTG), and sanukitoid: relationships and some implications for crustal evolution. *Lithos* **79**, 1-24.
- MATTE, P. (1991): Accretionary history and crustal evolution of the Variscan Belt in western Europe. *Tectonophysics* **196**, 309-337.
- MAURY, R.C., DEFANT, M.J. & JORON, J.L. (1992): Metasomatism of the sub-arc mantle inferred from trace-elements in Philippine xenoliths. *Nature* **360**, 661-663.
- MEHNERT, K.R. (1968): *Migmatites and the Origin of Granitic Rocks*. Elsevier, Amsterdam, The Netherlands.
- MENZIES, M.A., ROGERS, N.W., TINDLE, A. & HAWKESWORTH, C.J. (1987): Metasomatic and enrichment processes in lithospheric peridotites, an effect of asthenosphere–lithosphere interaction. In *Mantle Metasomatism* (M.A. Menzies & C.J. Hawkesworth, eds.). Elsevier, London, U.K. (313-361).
- MICHON, G. (1987): Les vaugnérîtes de l'Est du Massif Central français: apport de l'analyse multivariée à l'étude géochimique des éléments majeurs. *Bull. Soc. Géol. Fr.* **3**, 591-600.
- MONTEL, J.-M. (1993): A model for monazite/melt equilibrium and application to the generation of granitic magmas. *Chem. Geol.* **110**, 127-146.
- MONTEL, J.-M. & WEISBROD, A. (1986): Characteristics and evolution of “vaugneritic magmas”: an analytical and experimental approach, on the example of the Cévennes Médiannes (French Massif-Central). *Bull. Minéral.* **109**, 575-587.
- MOYEN, J.F., MARTIN, H. & JAYANANDA, M. (2001): Multi-element geochemical modelling of crust-mantle interactions during late-Archaean crustal growth: the Closepet granite (South India). *Precamb. Res.* **112**, 87-105.
- NELSON, K.D. (1992): Are crustal thickness variations in old mountain belts like the Appalachians a consequence of lithospheric delamination. *Geology* **20**, 498-502.
- NIXON, P.H., ROGERS, N.W., GIBSON, I.L. & GREY, A. (1981): Depleted and fertile mantle xenoliths from Southern African kimberlites. *Annu. Rev. Earth Planet. Sci.* **9**, 285-309.
- PAQUETTE, J.-L., MONCHOUX, P. & COUTURIER, M. (1995): Geochemical and isotopic study of a norite–eclogite transition in the European Variscan belt – implications for U–Pb zircon systematics in metabasic rocks. *Geochim. Cosmochim. Acta* **59**, 1611-1622.
- PATERSON, S.R., VERNON, R.H. & TOBISCH, O.T. (1989): A review of criteria for the identification of magmatic and tectonic foliations in granitoids. *J. Struct. Geol.* **11**, 349-363.
- PATIÑO DOUCE, A.E. & HARRIS, N. (1998): Experimental constraints on Himalayan anatexis. *J. Petrol.* **39**, 689-710.
- PATIÑO DOUCE, A.E. & JOHNSTON, A.D. (1991): Phase-equilibria and melt productivity in the pelitic system: implications for the origin of peraluminous granitoids and aluminous granulites. *Contrib. Mineral. Petrol.* **107**, 202-218.
- PEACOCK, S.M., RUSHMER, T. & THOMPSON, A.B. (1994): Partial melting of subducting oceanic-crust. *Earth Planet. Sci. Lett.* **121**, 227-244.

- PIN, C., BINON, M., BELIN, J.M., BARBARIN, B. & CLEMENS, J.D. (1990): Origin of microgranular enclaves in granitoids: equivocal Sr–Nd evidence from Hercynian rocks in the Massif-Central (France). *J. Geophys. Res.* **95**, 17821-17828.
- PIN, C. & DUTHOU, J.-L. (1990): Sources of Hercynian granitoids from the French Massif-Central – inferences from Nd isotopes and consequences for crustal evolution. *Chem. Geol.* **83**, 281-296.
- PIN, C. & LANCELOT, J. (1982): U–Pb dating of an Early Paleozoic bimodal magmatism in the French Massif Central and of its further metamorphic evolution. *Contrib. Mineral. Petrol.* **79**, 1-12.
- PIN, C. & PEUCAT, J.J. (1986): Age des épisodes de métamorphisme paléozoïque dans le Massif Central et le Massif Armoricain. *Bull. Soc. Géol. Fr.* **2**, 461-469.
- PLANK, T. & LANGMUIR, C.H. (1998): The chemical composition of subducting sediment and its consequences for the crust and mantle. *Chem. Geol.* **145**, 325-394.
- RAPP, R.P., SHIMIZU, N., NORMAN, M.D. & APPLGATE, G.S. (1999): Reaction between slab-derived melts and peridotite in the mantle wedge: experimental constraints at 3.8 GPa. *Chem. Geol.* **160**, 335-356.
- REINECKE, T. (1991): Very-high-pressure metamorphism and uplift of coesite-bearing metasediments from the Zermatt–Saas Zone, Western Alps. *Eur. J. Mineral.* **3**, 7-17.
- RHODES, J.M. & DAWSON, J.B. (1975): Major and trace element chemistry of peridotite inclusions from the Lashaine Volcano, Tanzania. *Phys. Chem Earth* **9**, 545-557.
- RUDNICK, R.L., McDONOUGH, W.F. & CHAPPELL, B.W. (1993): Carbonatite metasomatism in the northern Tanzanian mantle: petrographic and geochemical characteristics. *Earth Planet. Sci. Lett.* **114**, 463-475.
- SAWYER, E.W. (1998): Formation and evolution of granite magmas during crustal reworking; the significance of diatexites. *J. Petrol.* **39**, 1147-1167.
- SHAW, D.M. (1970): Trace element fractionation during anatexis. *Geochim. Cosmochim. Acta* **34**, 237-243.
- SIMIEN, F., MATTAUER, M. & ALLÈGRE, C.J. (1999): Nd isotopes in the stratigraphic record of the Montagne Noire (French Massif Central): no significant Paleozoic juvenile inputs, and pre-Hercynian paleogeography. *J. Geol.* **107**, 87-97.
- STORRE, B. & KAROTKE, E. (1972): Experimental-data on melting reactions of muscovite + quartz in systems  $K_2O-Al_2O_3-SiO_2-H_2O$  to 20 kb water pressure. *Contrib. Mineral. Petrol.* **36**, 343-345.
- STRECKEISEN, A. (1976): To each plutonic rock its proper name. *Earth-Sci. Rev.* **12**, 1-33.
- SUN, S.S., McDONOUGH, W.F., SAUNDERS, A.D. & NORRY, M.J. (1989): Chemical and isotopic systematics of oceanic basalts; implications for mantle composition and processes. In *Magmatism in the Ocean Basins* (A.D. Saunders & M.J. Norry, eds.). *Geol. Soc., Spec. Publ.* **42**, 313-345.
- TAYLOR, S.R. & McLENNAN, S.M. (1981): The composition and evolution of the continental-crust – rare-earth element evidence from sedimentary rocks. *Philos. Trans., R. Soc. London, Ser. A* **301**, 381-399.
- TAYLOR, S.R. & McLENNAN, S.M. (1985): *The Continental Crust: Its Composition and Evolution*. Blackwell, Oxford, U.K.
- THOMPSON, A.B. & CONNOLLY, J.A.D. (1995): Melting of the continental crust: some thermal and petrological constraints on anatexis in continental collision zones and other tectonic settings. *J. Geophys. Res.* **100**, 15565-15580.
- TURPIN, L., VELDE, D. & PINTE, G. (1988): Geochemical comparison between minettes and kersantites from the western European Hercynian orogen: trace-element and Pb–Sr–Nd isotope constraints on their origin. *Earth Planet. Sci. Lett.* **87**, 73-86.
- VANDERHAEGHE, O. (2001): Melt segregation, pervasive melt migration and magma mobility in the continental crust; the structural record from pores to orogens. *Phys. Chem. Earth* **26**, 213-223.
- VANDERHAEGHE, O., BURG, J. & TEYSSIER, C. (1999): Exhumation of migmatites in two collapsed orogens: Canadian Cordillera and French Variscides. In *Exhumation Processes: Normal Faulting, Ductile Flow and Erosion* (U. Ring, M.T. Brandon, G.S. Lister & S.D. Willet, eds.). *Geol. Soc., Spec. Publ.* **154**, 181-204.
- VAN DER WAL, D. & BODINIER, J.-L. (1996): Origin of the recrystallisation front in the Ronda peridotite by km-scale pervasive porous melt flow. *Contrib. Mineral. Petrol.* **122**, 387-405.
- VENTURELLI, G., CAPEDEI, S., DIBATTISTINI, G., CRAWFORD, A., KOGARKO, L.N. & CELESTINI, S. (1984): The ultrapotassic rocks from southeastern Spain. *Lithos* **17**, 37-54.
- VERNON, R.H. (1984): Microgranitoid enclaves in granites – globules of hybrid magma quenched in a plutonic environment. *Nature* **309**, 438-439.
- VERNON, R.H. (1986): K-feldspar megacrysts in granites – phenocrysts, not porphyroblasts. *Earth-Sci. Rev.* **23**, 1-63.
- VERNON, R.H., WILLIAMS, V.A. & DARCY, W.F. (1983): Grain-size reduction and foliation development in a deformed granitoid batholith. *Tectonophysics* **92**, 123-145.
- VIELZEUF, D. & HOLLOWAY, J.R. (1988): Experimental determination of the fluid-absent melting relations in the pelitic system – consequences for crustal differentiation. *Contrib. Mineral. Petrol.* **98**, 257-276.

- WATSON, E.B., VICENZI, E.P. & RAPP, R.P. (1989): Inclusion/host relations involving accessory minerals in high-grade metamorphic and anatectic rocks. *Contrib. Mineral. Petrol.* **101**, 220-231.
- WIEBE, R.A. (1968): Plagioclase stratigraphy; a record of magmatic conditions and events in a granite stock. *Am. J. Sci.* **266**, 690-703.
- WIEBE, R.A. & COLLINS, W.J. (1998): Depositional features and stratigraphic sections in granitic plutons: implications for the emplacement and crystallization of granitic magma. *J. Struct. Geol.* **20**, 1273-1289.
- WINTERBURN, P.A., HARTE, B. & GURNEY, J.J. (1990): Peridotite xenoliths from the Jagersfontein kimberlite pipe. 1. Primary and primary-metasomatic mineralogy. *Geochim. Cosmochim. Acta* **54**, 329-341.
- WYLLIE, P.J. (1987): Metasomatism and fluid generation in mantle xenoliths. *In* Mantle Xenoliths (P.H. Nixon, ed.). J. Wiley & Sons, New York, N.Y. (609-621).

*Received July 26, 2005, revised manuscript accepted September 13, 2006.*